

Extinction drives recent thermophilization but does not trigger homogenization in forest understory

Jeremy Borderieux^{1, *}, Jean-Claude Gégout¹, Josep M. Serra-Diaz^{1, 2}

1. Université de Lorraine, AgroParisTech, INRAE, UMR Silva, 54000 Nancy, France
2. Eversource Energy Center and Department of Ecology and Evolutionary Biology, University of Connecticut, Storrs, CT, United States of America

Corresponding author: Jeremy Borderieux: jeremy.borderieux@agroparistech.fr

Abstract

The ongoing climate change is triggering plant community thermophilization. This selection process is ought to shift community composition toward species adapted to warmer climates but may also lead to biotic homogenization. The link between thermophilization and homogenization, and the community dynamics that drive them (colonization and extinction) remain unknown, but is critical for understanding community responses under rapid environmental change.

We used 14,167 pairs of plots to study shifts in plant community during 10 years of rising temperature, in 80 forest ecoregions of France. We computed community mean thermal optimum (thermophilization) and $\Delta\beta$ -diversity (homogenization) for each ecoregion and partitioned these changes into extinction and colonization dynamics of cold- and warm-adapted species.

Forest understory communities thermophilized on average by $0.12\text{ }^{\circ}\text{C decade}^{-1}$ and up to $0.20\text{ }^{\circ}\text{C decade}^{-1}$ in warm ecoregions. This rate was entirely driven by extinction dynamics. Extinction of cold-adapted species was a driver of homogenization, but it was compensated for by the colonization of rare species and the extinction of common species, resulting in the absence of an apparent homogenization trend.

Here we show a dieback of present cold-adapted species rather than an adaptation of communities via the arrivals of warm-adapted species, with mutually cancelling effect on β -diversity. These results suggest that a future loss of biodiversity and delayed biotic homogenization should be considered.

Keywords

Community ecology, thermophilization, homogenization, β -diversity, climate change, forest, understory.

1. Introduction

The unprecedented speed of current climate warming is causing major species range shifts and the reshuffling of ecological communities (Franklin et al., 2016; Lenoir & Svenning, 2015; Svenning & Sandel, 2013). This reshuffling could lead to a major risk for biodiversity (Sala et al., 2000) and the services it provides (Reu et al., 2022; Wang et al., 2021). Two major patterns of community composition have been reported as a result of global change, namely thermophilization and biotic homogenization. On the one hand, thermophilization of plant communities - the increase of the average temperature affiliation of species in a community over time - is occurring as a result of climate warming (De Frenne et al., 2013; Martin et al., 2019; Richard et al., 2021), yet at a slower pace than climate change (Bertrand et al., 2011, 2016). On the other hand, evidence also suggests that biotic homogenization across plant communities is taking place (Cholewińska et al., 2020; Olden & Rooney, 2006; Staude et al., 2022). This is shown by a decrease in β -diversity, which signals an increase of similarity among the communities of a region. To date, we do not know whether these two processes occur simultaneously, what their linkages are, and which community dynamics underlie them.

Baseline expectations from global warming suggest that warm-adapted species may increasingly replace cold-adapted species in communities (De Frenne et al., 2013; Gottfried et al., 2012; Svenning & Sandel, 2013). At large scales, biogeographic theory predicts species range shifts (Lenoir & Svenning, 2015) but lagged dynamics, controlled by the dispersal and establishment capacities of species that may constrain the maximum speed at which , species can colonize suitable climatic areas. (Boulangeat et al., 2012; Govaert et al., 2021; Ozinga et al., 2009). Thus, thermophilization is the product of different rates of colonization and/or extinction (*sensu* local extinction, Leibold et al., 2004) of warm- vs. cold-adapted species in a community. At one end, thermophilization may stem from colonization of warm-adapted species without any extinction of cold-adapted species (Fig.1). Conversely, thermophilization may exclusively stem from extinction of cold-adapted species, implying biotic erosion of communities rather than colonization of species adapted to warmer climate (Fig.1). For instance, extinction-driven thermophilization is expected in Mediterranean communities of Europe, where many temperate species are located at the warm edge of their distribution. As a result, they are subject to extirpation by drought and heat waves, without being replaced by warmer-adapted species as the sea may act as a barrier for colonization (Bertrand et al., 2016; Pérez-Navarro et al., 2021).

Thermophilization is being increasingly detected, but little is known about how it could affect β -diversity. Both local (α) diversity and β -diversity are increasing in mountain forests and on summits, where colonization of unoccupied space by new species increases the regional species pool (Bahn & Körner, 2003; Steinbauer et al., 2018). However, lowland forests are showing signs of homogenization (Cholewińska et al., 2020; Tobias & Monika, 2012; Xu et al., 2023; Zwiener et al., 2018). By selecting species as a function of their thermal tolerance, thermophilization could decrease β -diversity. For example, it could promote already widespread warm-adapted species, increasing redundancy between communities (Fig.1.b, Dietz et al., 2020; Dupouey et al., 2002; Fischer et al., 2002). As species rarity is linked to environmental specialization (Crisfield et al., 2023), thermophilization could also lower β -diversity by removing specialized cold-adapted species (Fig.1.b). This process is not unidirectional: an increase in temperature can also relieve cold constraints on rare specialized warm-adapted species and increase β -diversity. Finally, thermophilization can induce differentiation between communities by reducing the occurrence of widespread species (without causing definitive removal), as frequently observed at the beginning of an anthropogenic stress (Socolar et al., 2016). These multifaceted links between climate-change-induced thermophilization and homogenization highlight the need to disentangle the community dynamics at play (Baeten et al., 2012; Gosselin, 2016).

We aimed to unveil the community dynamics (local extinction and colonization) involved in thermophilization and β -diversity shifts. We disentangled the β -diversity and thermophilization dynamics based on recent methods to separate the extinction and colonization processes of temporal changes in communities (Tatsumi et al., 2021). We analyzed temporal shifts from 2005 to 2021 in 14,167 pairs of plots (“past” and “recent” plots form spatially proximate (<2 km) pairs of plots) of understory forest communities spanning 756 plant species in 80 forest ecoregions. These ecoregions are homogenous in environmental conditions and cover the French continental area (529,772 km²; 172,080 km² of forested area). We computed the individual contribution of each species to the changes in mean thermal optima (i.e. thermophilization) and β -diversity (i.e. homogenization) in each ecoregion (Fig1.b). We partitioned these contributions into 4 community processes: extinction and colonization (decline or gain in occurrences) of cold- and warm-adapted species (relative to the baseline mean thermal 2005-2011 optimum).

In this study we aimed at understanding such community processes by responding to these questions: (1) Is there a recent significant thermophilization of forests, and what

community processes drive it? (2) Is there a significant flora homogenization of forests occurring, and what community processes drive it? And (3) is mean annual temperature significantly linked to thermophilization and homogenization and to the extinction and colonization processes? Our initial expectation was that i) thermophilization is a product of both extinction of cold-adapted species and colonization by warm-adapted species, and ii) homogenization is pervasive and triggered by abundant colonization by warm-adapted species and extinction of rare cold-adapted species. We expected faster thermophilization rates in Mediterranean ecoregions because more species could be located at the warm edge of their distribution and prone to local extinctions caused by extreme (drought) events (Pérez-Navarro et al., 2021).

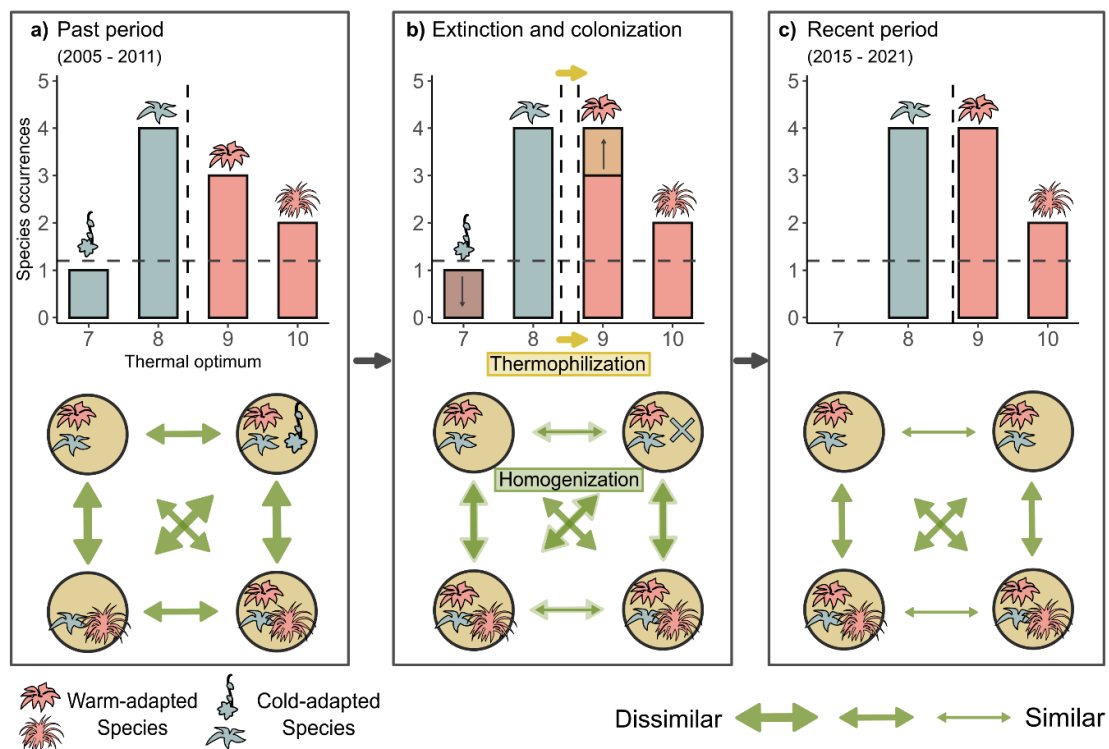


Figure 1: Example of the coupling of thermophilization and homogenization under increasing temperature: a) Artificial ecoregion composed of four communities. The ecoregion has two cold- and two warm-adapted species depending on whether their thermal optimum is lower or higher than the mean thermal optimum of the ecoregion. The communities are heterogenous because they all have unique species composition. The vertical dotted line represents the weighted mean thermal optimum of every species (of the ecoregion); the horizontal dotted line represents the threshold differentiating rare from common species. b) Example of thermophilization triggered by the spread of a warm-adapted species and the extinction of a cold-adapted species. The loss of a rare species that made the community unique triggers homogenization, and so does the spread of a common species by increasing similarity between communities (the arrow width shrinks). Thermophilization can also heterogenize communities by removing common cold-adapted species or promoting a rare or previously absent warm-adapted species (not shown). c) Resulting ecoregion with a higher mean thermal optimum and more similar communities.

2. Results & Discussion

Extinction of species drives thermophilization

The declines in species occurrences (15,996 lost occurrences) outweighed species expansion (8,822 new occurrences, $n_{\text{plots}} = 14,167$ pairs of plots, 2005-2011 vs. 2015-2021, Fig.2). Extinction was preponderant for the relatively cold-adapted species, and colonization was dominant for the relatively warm-adapted species (Fig.2). As a consequence, 72 out of the 80 ecoregions had a positive thermophilization rate. The mean thermophilization rate of an ecoregion was $0.012 \text{ } ^\circ\text{C yr}^{-1}$ (s.d. 0.011, Fig.3.a), entirely driven by extinction (Fig.3.a) - local extinction, defined as species with occurrences decreasing over time. Even if occurrences of species were gained (Fig.2), colonization did not contribute significantly to thermophilization (Fig.3.a) because the gains were lesser in comparison to the losses, and the gained species did not have higher thermal optima than the mean of the ecoregion to contribute to thermophilization. The use of proximate plots instead of resurveyed plots, and the sometime low number of plots within ecoregions resulted in high standard deviations. Our interpretation however, did not vary when weighting our mean values by the number of plots within an ecoregion (see Methods section). The thermophilization rate was consistent with previous studies on flora changes in temperate forest understory (Bertrand et al., 2011; Dietz et al., 2020; Govaert et al., 2021; Martin et al., 2019; Richard et al., 2021), that reported rates of *ca.* $0.010 \text{ } ^\circ\text{C yr}^{-1}$, lower than the observed warming rate of *ca.* $0.026 \text{ } ^\circ\text{C yr}^{-1}$ in our study region (Dietz et al., 2020).

Thermophilization is generally interpreted as the gradual replacement of cold-adapted species by warm-adapted species, whose growth and establishment are facilitated by increased temperature (De Frenne et al., 2013). We only found evidence for an extinction dynamic (e.g. decrease in occurrence rates) driving thermophilization, with a contribution of $0.012 \text{ } ^\circ\text{C yr}^{-1}$ (s.d. 0.009), equal to the total observed thermophilization rate. This result was confirmed by a null model in which the change in the occurrences of a species was independent of its thermal optimum. This null model displayed a contribution of extinction to thermophilization not significantly different from 0 (Fig.3.a, Extended Fig.1, see “Null models” in Methods section). As our study started in 2005, a preexisting disequilibrium between flora and climate may have induced a greater contribution of extinction, induced by the extirpation of already stressed individuals in addition to those that underwent the recent warming from 2005 and onward. Our method does not distinguish these two kinds of extirpations. However, the rates we found remain indicative of the recent effect of warming on communities, as extinction of already stressed species is an integral part of

thermophilization (Pérez-Navarro et al., 2021). Conversely, the observed effects of colonization on thermophilization were not significantly different from the random rates of the null model (Fig.3.a). Our results and interpretation of extinction-driven thermophilization were consistent when using a different species thermal optimum database (EcoPlant, Gégout et al., 2005, Table S1). We also rejected the hypothesis of overall decreases of occurrences or sampling pressure (Fig.2) as explanations for the significance of the contribution of extinction with a rarefaction model - in which the two time frames of an ecoregion have an equal number of total occurrences (Table S2, see “Null models” in Methods section).

Extinction has already been identified as a key driver of thermophilization in drylands (Pérez-Navarro et al., 2021), *via* the selection of the most drought-resistant species at the expense of the colder-adapted species after a drought-pulse event. Our results extend this observation to the European temperate, Mediterranean and mountainous forest biomes (Extended Fig.2) over 16 years of continued warming. The Mediterranean and the warmest lowland ecoregions experienced the fastest thermophilization rates. We estimated that the contribution of extinction increased by $0.003\text{ }^{\circ}\text{C yr}^{-1}$ *per* degree Celsius rise in mean annual temperature (Fig.4.a), and up $0.020\text{ }^{\circ}\text{C yr}^{-1}$ in the southernmost ecoregions (Fig.4.a). This higher local extinction rate indicates that thermal stress under warmer climate conditions is sufficient to trigger the mortality of cold-adapted individuals or impair their establishment. This finding concurs with projections of species climatic suitability, which predict extinctions at the warm edge of the range of the species distribution, where their maximum tolerance is expected to be exceeded first (Dullinger et al., 2012; Engler et al., 2011; Kuhn & Gégout, 2019). Our occurrence-based analysis did not account for species abundance or interspecific competition. However, as warm-adapted species could thrive under a warmer climate, their competitive abilities also increase, and this impairs the survival of cold-adapted species (Sanczuk et al., 2022; Staude et al., 2022).

The thermophilization rates found in the present study do not match the climate warming rates over the study period ($0.026\text{ }^{\circ}\text{C yr}^{-1}$ on average, Dietz et al., 2020), implying a delay between climate change and shifts in the community dynamics. This discrepancy could be explained by the absence of colonizing warm-adapted species speeding up thermophilization. As our analysis was at the ecoregion scale, our results (Fig.4.a) are in line with the expected colonization debt of understory plants over large homogenous climate areas (Bertrand et al., 2011). The absence of colonization is likely a consequence of climate being only one of the many drivers of plant dispersal and establishment. The increase of the establishment and growth rates of warm-adapted species benefiting from climate change does not compensate for the limited dispersal capacities of plants

(depending on their life cycle, seed traits, etc.) that are not fast enough to follow isotherm shifts induced by climate warming in lowland ecosystems (Lenoir & Svenning, 2015; Loarie et al., 2009; Serra-Diaz et al., 2014). The only ecoregions where the contribution of colonization significantly drives thermophilization (yet by no more than a third) are the mountainous ecoregions (Extended Fig.2; see also Bertrand et al., 2011; Lenoir et al., 2008), where the distance to track shifting isotherms is shorter than in lowlands (Rolland, 2003) and facilitates colonization. Other explanatory factors could stem from local adaptation of plant populations (Franks et al., 2014; Kubisch et al., 2013; Lavergne et al., 2010) and forest microclimates (De Frenne et al., 2019). Temperature buffering by the forest canopy slows down thermophilization by reducing the exposure of cold-adapted species to stress and extreme events (De Frenne et al., 2019; De Lombaerde et al., 2021; Suggitt et al., 2018; Zellweger et al., 2020). Denser canopy and forest succession also exclude warm- and light-demanding species, thus slowing down thermophilization (Bergès et al., 2013; Bodin et al., 2013). Therefore, our results are conservative in the face of increasing forest microclimatic buffering via canopy cover, and the exclusion of warm-adapted species by forest succession. We found a no significant correlation between thermophilization and basal area, and a significant but weak correlation (5.0% R^2) between thermophilization and increment canopy cover (Fig.S2). These results confirm that the thermophilization signal is robust and not dependent on forest maturation.

Absence of large-scale community homogenization

We expected the ecoregion to homogenize toward warmer-adapted communities, in line with the strong signal of extinction-driven thermophilization (Fig.1). However, homogenization was not a general trend: only 37 out of the 80 ecoregions displayed a negative $\Delta\beta$ -diversity (Whittaker B_w diversity - see Methods section), whereas 43 showed a positive one. The mean β -diversities of the ecoregions were 12.8 (s.d. 3.7, $n=80$) in the past period and 13.1 (s.d. 3.8) in the recent period. The mean $\Delta\beta$ -diversity across ecoregions was 0.29 (s.d. 1.4, $n=80$) and was not significantly different from 0 (Fig.3.b). Whittaker B_w -diversity index is a measure of homogeneity as it allows to infer γ -diversity (the number of species of the ecoregion) by multiplying the local diversity (α) by B_w .

The absence of a clear trend in homogenization did not imply a stasis of the community dynamics. We found significant contributions from the colonization of warm- and cold-adapted species relatively to the mean optimum of the ecoregion and from the extinction of cold-adapted species (Fig.3.b) to changes in β -diversity. These dynamics displayed opposite directions and cancelled each other out, resulting in an overall weak signal of community homogenization. The colonization dynamics contributed significantly to

heterogenization (mean effect 1.08, s.d. 0.97, Fig.3.b). This implies that the heterogenization effect of colonization by rare or new species outweighed the homogenization (β -diversity decrease) caused by the increase of already widespread species. Surprisingly, this effect was explained by colonization of cold-adapted species (Fig.3.b, 0.87, s.d. 0.71). As no significant increase of cold-adapted species was detected in the thermophilization analysis (Fig.2), this positive contribution is explained by stochastic colonization by rare or previously absent cold-adapted species. The unpredictability of such events may arise from extreme but exceptional values of the dispersal distance of some species (Vittoz & Engler, 2007), dormant seeds in the seedbank (Gasperini et al., 2021), but also from the limited number of plots in certain ecoregions. With a low number of plots, γ -diversity (the total number of species in the ecoregion) is lower, so that the species partitioning methods are more sensitive to local colonization by rare species that affects γ -diversity.

Extinction of cold-adapted species - the main driver of community thermophilization (see above) - significantly contributed to homogenization (-0.74, s.d. 0.82, Fig.3.b). However, the extent of this contribution was comparable to the colonization effect. To better understand the contributions of extinction and colonization, we partitioned them into “rare” and “common” species contributions. Species present in less than 10% of the baseline plots were deemed rare. This further partitioning showed that the decline of rare cold-adapted species strongly contributed to homogenization (-1.73, Extended Fig.3) but was mitigated by simultaneous gains in heterogeneity caused by the decline of common cold-adapted species (0.99, Extended Fig.3). Although the effect of common cold-adapted species on $\Delta\beta$ -diversity was lower, it should not be overlooked because it corresponds to species contributing to two thirds of thermophilization (Extended Fig.3). Furthermore, the decline of widespread cold-adapted species offset the extinction of rare cold-adapted species by reducing local diversity and increasing heterogeneity between plots.

Our results likely reflect transient community dynamics where a new anthropogenic stressor initially increases β -diversity by reducing the occurrences of widespread species but is not acute enough to trigger definitive species extinction (as opposed to the local extinctions measured here). This first increase in β -diversity could be temporary: all species would become rarer over time, and eventually become extinct (Socolar et al., 2016). In our case, the contribution of the decline of rare cold-adapted species to homogenization outweighed the positive effect of its colonization counterpart. That is, the number of declining rare species was higher than the number of colonizing rare species. In addition to

the thermal stress imposed by climate change, populations of rare species are likely to be isolated from their source population and lack the critical size for population survival (Leibold & Chase, 2017; Pérez-Navarro et al., 2021). Competition with ubiquitous species could also play a role in the decline of rare species, but only a further analysis with abundance-based surveys and β -diversity estimates could disentangle the local dynamics driving homogenization. We used a rarefaction null model keeping α -diversity constant to test the sensitivity of β -diversity estimates to the sampling intensity. This model revealed that a decrease in sampling intensity increased β -diversity, likely because common species are less sampled. Therefore, our results and the potential observation of homogenization are robust to decreases in occurrences, whether real or resulting from the sampling intensity.

The different contributions to homogenization depending on the relative thermal optima of species are indicative of the relationship between thermophilization and β -diversity. Thermophilization is a selective process documented in the present study as a decline of cold-adapted species alongside an antagonistic effect on β -diversity. The homogenization components, e.g. thermophilization, are correlated with the mean annual temperature of each ecoregion (Fig.4). The higher sensitivity of $\Delta\beta$ -diversity to extinction in the southernmost Mediterranean ecoregions highlights a faster turnover of communities, which causes risks of homogenization if the decline of rare and common species alike continues.

Implications for forest understory in a warming climate

Thermophilization is often viewed as the process that leads to communities composed of species adapted to warmer conditions (De Frenne et al., 2013; Gottfried et al., 2012), but our results show that it can also stem from local extinctions of cold-adapted species, with little substitution by warm-adapted species. Our study evidences a lack of persistence of understory plant species concurrent with rising temperature and exceeding the establishment and dispersal capacities of plants better adapted to warmer climates. The discrepancy between communities and climate is often referred to as a climatic debt (Devictor et al., 2012). Our study illustrates that extinction-driven thermophilization is the consequence of the “repayment” of this debt (Jackson & Sax, 2010). These extinctions threaten the ecosystem services that the herbaceous layer and its diversity provide (Landuyt et al., 2019; Mori et al., 2018; Tobias & Monika, 2012; Wang et al., 2021).

Further research and the use of different methods could add insights to our results. The presence/absence methods used here are indicative of the large-scale changes in

species composition, but they do not capture changes in local abundances. The use of abundance-based metrics could reveal ongoing homogenization through the local spread of warm-adapted species despite low new plot colonization or local hotspots by rare species that ultimately decrease the homogenization risk (Tatsumi et al., 2022). Climate-driven reshuffling is not the only potential source of homogenization. Processes like nitrogen deposition, agriculture intensification, and forest succession all introduce and favor certain species and could create redundancy in communities (Danneyrolles et al., 2021; Heinrichs & Schmidt, 2017; Merle et al., 2020; Staude et al., 2022). These processes could act in synergy with climate change, and need to be further analyzed in future homogenization studies because they can be partly confounded in our results. Our partitioning analysis isolated the effect of the decline of cold-adapted species - a dynamic less impacted than colonization by the aforementioned process and limited the risk of misinterpretation.

Our consistent finding of extinction being the driver of thermophilization calls for increased needs to assess future biodiversity trends. In other ecosystems, where the spread of warm-adapted species can be faster than in forests, the effects of β -diversity should keep being studied and monitored (Staude et al., 2022; Xu et al., 2023). We demonstrated that the extinction of cold-adapted species occurs independently of their rarity, and partitioning detected opposed dynamics hidden behind a seeming absence of trend. The decline of rare species is pervasive and hard to detect without dedicated conservation studies, but widespread cold-adapted species could be used to bioindicate early signs of climate-induced extinctions. The question of whether increased thermophilization and the absence of homogenization are transient and respond to the current flora-climate disequilibrium will need further monitoring but remains critical to preserve biodiversity. Explicitly unveiling the community dynamics at play will strengthen our capacity to understand and predict community compositions under an accelerating warming rate.

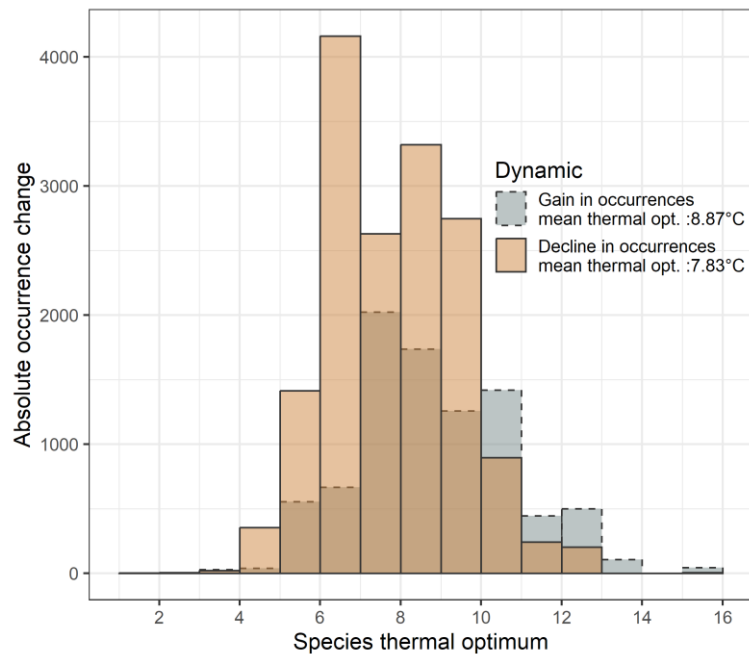


Figure 2: Absolute changes in species occurrences according to their thermal optima. Changes in species occurrences between the 14,167 “past” plots (surveyed in 2005-2011) and 14,167 “recent” plots (surveyed in 2015-2021). The absolute occurrence change was computed by summing every species occurrence change between the “recent” and “past” plots separately for declining (i.e. extinction, less occurrences in “recent” plots) and spreading (i.e. colonization, more occurrences in “recent” plots) species and for each 1 °C thermal optimum class. The weighted (by absolute occurrence changes) means of the species thermal optima are also displayed. The thermal optimum of a species is estimated as the mean of the mean annual temperatures within the distribution range of a species (Vangansbeke et al., 2021).

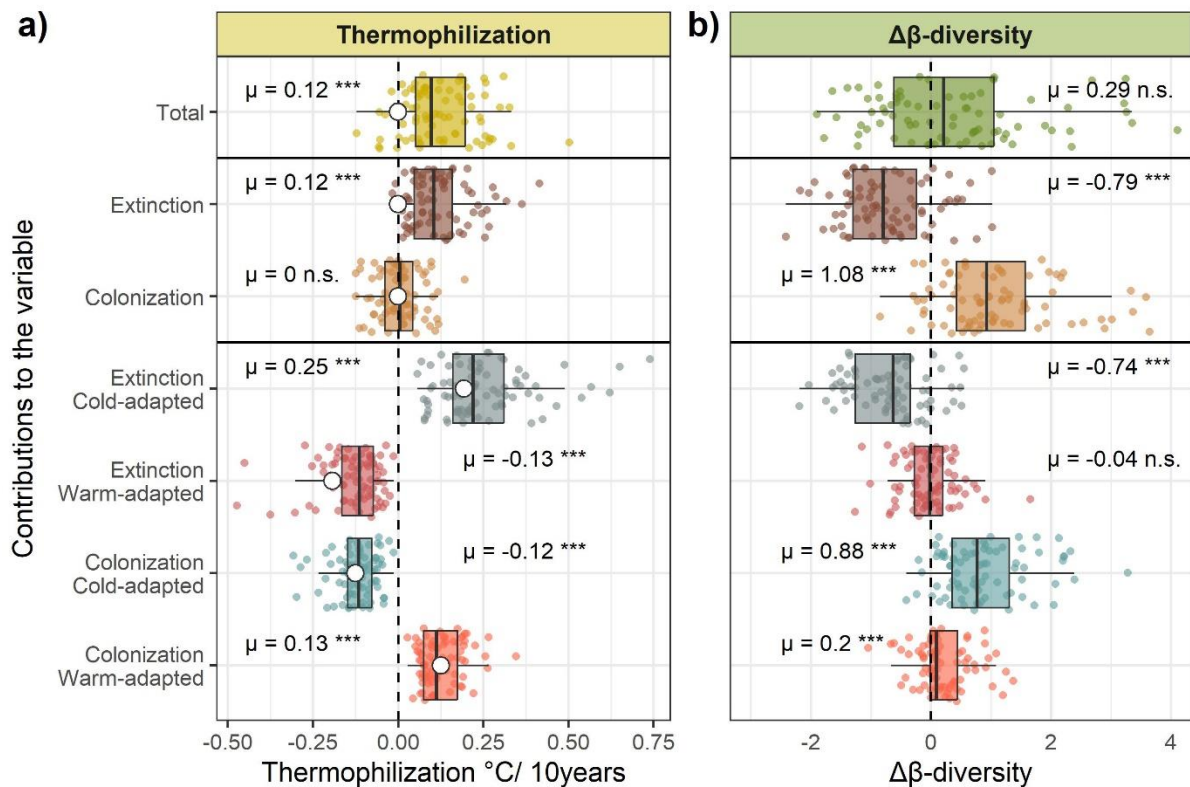


Figure 3: Community dynamics partitioning of thermophilization (a) and homogenization (b). Each dot represents the values of one of the 80 ecoregions ($n=80$). Changes in the mean thermal optima a) of the recorded species and b) in β -diversity (thermophilization and $\Delta\beta$ -diversity, respectively) in the 80 ecoregions. The changes are broken up in two components - colonization and extinction - estimated from the contributions of species with more/less occurrences in the recent period. These components were subsequently divided into the contributions of relatively cold- or warm-adapted species, defined as species with a lower or higher thermal optimum than the mean thermal optimum of the ecoregion in the past period. For each component, the mean value is displayed ($^{\circ}\text{C decade}^{-1}$ for thermophilization, no unit for $\Delta\beta$ -diversity). White dots, mean value of the null thermophilization model. The statistical differences between these means and the means of a null model, obtained with a two-sided Wilcoxon test (for thermophilization) or 0 (for $\Delta\beta$ -diversity) are also displayed; $p<0.05$ (*), $p<0.01$ (**), $p<0.001$ (***). Exact P-values are available in Table S1. Boxes, 25th centile, median, and 75th centile; whiskers do not extend further than 1.5 times the interquartile range. One outlier ecoregion is not displayed in b) because a low number of plots yielded a $\Delta\beta$ -diversity value of -5.2.

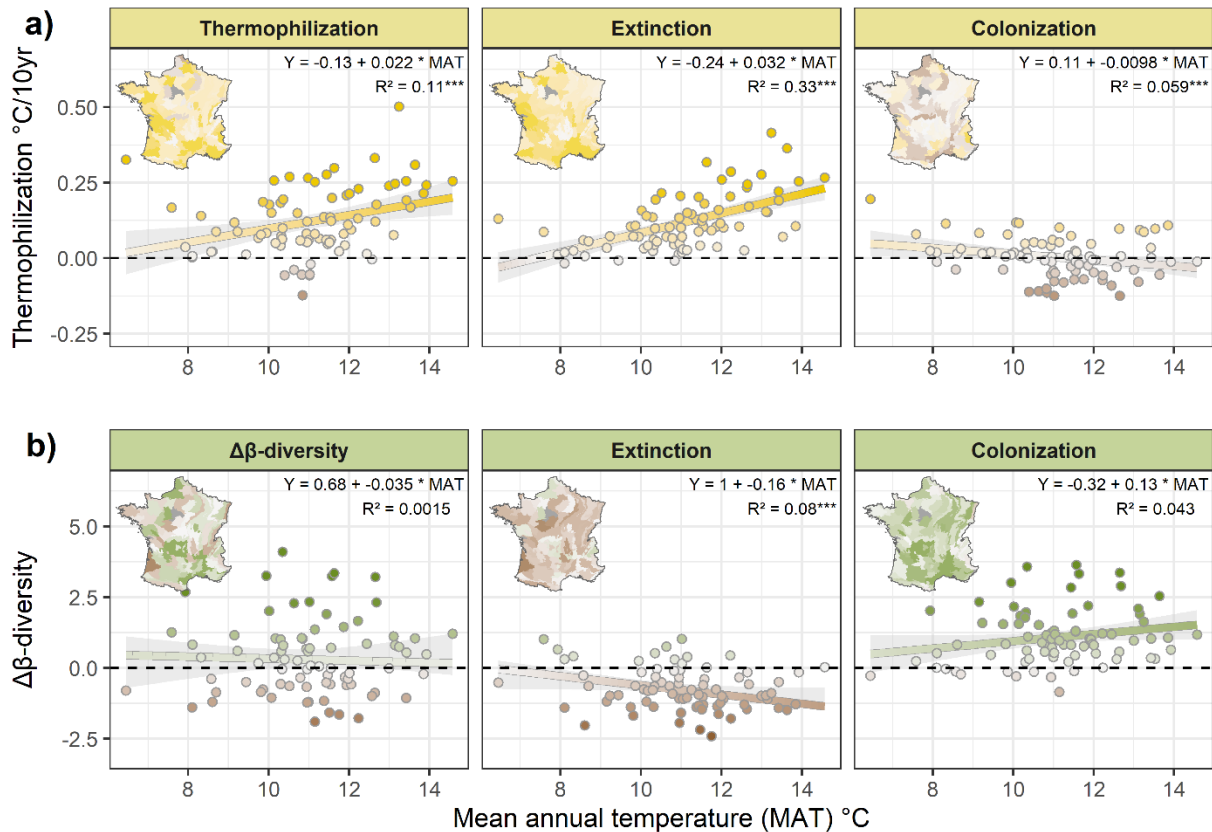


Figure 4: Relationship between i) thermophilization (a), β -diversity changes (b) and their extinction and colonization components, and ii) mean annual temperature (MAT). One point represents one ecoregion, the map of the ecoregion with the associated value is displayed for each component (n=80). The color scale of the points and the mapped ecoregions are the same and refer to the Y axis (thermophilization or $\Delta\beta$ -diversity). The summary statistics corresponds to a linear model value \sim MAT. (*) significant MAT coefficient. One outlier ecoregion is not displayed in (b), because a low number of plots yielded a $\Delta\beta$ -diversity value of -5.2. The error band represents the confidence interval of the linear model.**

3. Materials and methods

Study region and forest ecoregion

The study area corresponded to metropolitan France (excluding Corsica island), including the temperate mixed forest biome, the coniferous mountain biome and the Mediterranean forest biome. The territory was divided into 83 forest ecoregions (called “ecoregions” hereafter) characterized by similar and unique combinations of climatic and soil conditions (IGN, 2013). We used these ecoregions to delineate sampling areas and study understory flora changes and diversity at a wider scale than the plot scale. As the ecoregions displayed distinct climate and soil characteristics, we assumed that the pool of species was similar within an ecoregion but differed from the pools of the other ecoregions.

Lowland ecoregions were characterized by mosaics of forest, meadow, and cropland, with a climate ranging from oceanic to semi-continental (mean annual temperature ranges from 9.4 to 13.9 °C at the ecoregion scale and precipitation ranges from 500 to 1,800 mm yr⁻¹). Mountainous and pre-mountainous ecoregions displayed a greater forest cover and a continental mountainous climate, except oceanic influence on the Pyrenees (mean annual temperature range 6.5 to 12.4 °C, precipitation range 400 to 2,000 mm yr⁻¹). The southernmost ecoregions encompassed the Mediterranean border from Spain to Italy and displayed the warmest and driest climate of European France (mean annual temperature range 11.6 to 14.6 °C, precipitation range 284 to 451 mm yr⁻¹) (IGN, 2013).

Plot selection

We extracted data from the recent protocol of the French National Forest Inventory (NFI), started in 2005. We selected the plots from 2005 to 2021. The systematic sampling of the NFI is based on 1km-by-1km grid, with one tenth of the grid nodes surveyed each year. Once the grid is completely surveyed, a new survey cycle starts, approximately 10 years later. The plots of the new cycle are not a revisit of the previous plots but a new plot proximal to the node. We extracted the mean annual temperature (MAT) of each plot from a climate model calibrated with 214 French weather stations over the 1990-2015 period (Piedallu et al., 2019) and elevation from a 25-m resolution digital elevation model.

We took advantage of the spatial representativeness offered by the systematic sampling to study vegetation changes by creating a dataset balanced in sampling intensity and along environmental conditions over time. We assigned the plots from the 2005-2011 campaign to the “past” category and the plots from the 2015-2021 campaign to the “recent” category. Plots in-between these two timeframes were removed because their nearest plot counterpart from the new cycle (planned for 2022-2024) was not available yet. We also removed the plots identified as deforested at the time of the survey and the plots with less than five species with a known thermal optimum. Our analysis (described below) was performed at the ecoregion scale by pooling all the plots of an ecoregion to reduce the variability that geographically close (but not revisited) plots would have induced.

Then, we paired “past” and “recent” plots based on several criteria: (1) a distance between two plots < 2 km, (2) a time interval of 9, 10 or 11 years between plots, (3) plots located in the same ecoregion, (4) a difference in the elevations of two plots < 50 m. Criterion (1) allowed us to select plots from two NFI cycles belonging to the same node, and compensate for the low precision of the coordinates of the NFI plots (\pm 500m) due to private property protection laws. Furthermore, we removed three ecoregions with low numbers (N<10) of pairs from the initial 83 ecoregions.

The selection procedure yielded 14,167 pairs of NFI plots separated on average by 9.9 years (Extended Fig.4), distributed in 80 ecoregions. The ecoregions had a minimum of 15 pairs and a maximum of 1,892 pairs (median 118). In the absence of true remeasurements of past surveys, the selection of geographically close plots to study vegetation changes was the best alternative, but could misestimate or detect non-existing changes (Chytrý et al., 2014). However, by conducting 80 separate flora change analyses - one *per* ecoregion - we identified consistent trends across ecoregions, and averaging the results limited the risk of misinterpretation. Furthermore, 33 ecoregions had less than 100 plot pairs (Extended Fig.4), so that the results from those ecoregions could be interpreted with caution. However, by weighting the means presented in Fig.3 by the number of pairs of each ecoregion, we found no significant difference in our interpretation. Therefore, the number of plot pairs in the ecoregions did not influence the results.

Floristic database

In addition to the dendrometric, canopy cover and soil measurements, the NFI includes floristic surveys performed in 15-m-radius circles (area = 709 m²). Based on these surveys, we selected vascular plants identified to the species level, and removed trees because their presence in the understory can result from forest management and they respond slowly to environmental changes (Lenoir et al., 2008). After homogenization of the taxonomy to the TaxRef V13 standard (Gargominy, 2022), we assigned a thermal optimum from the ClimPlant V1.2 database (Vangansbeke et al., 2021) to each species. The thermal optima were computed by averaging the mean annual temperature within the species distribution range obtained from European atlases. We also extracted two additional thermal optima (one computed in 2005 and one computed in 2019 with updated information and methods) based on EcoPlant (Gégout et al. 2005) to test the sensitivity of our results to the source information of thermal optimum estimation. The EcoPlant database compiles French floristic (presence-absence) surveys that allow calibrating an optimal probability of presence along a 1km climatic grid. EcoPlant and ClimPlant are complementary: the ClimPlant database captures the whole climatic gradient of a species distribution range, whereas the EcoPlant database is limited by the French border but is built from detailed surveys and a high-resolution climatic model (Piedallu et al., 2019) that enables an accurate estimation of thermal optima.

We recorded 202,866 species occurrences in the past plots, and 195,692 species occurrences in the recent plots. Out of our initial 1,622 species, we matched 756 species with a known thermal optimum from ClimPlant V1.2. These occurrences represented 78% of the total

number of occurrences recorded in our plot pairs, showing a large taxonomic coverage of the thermal optimum database.

Computation and partitioning of thermophilization

To compute thermophilization, we first defined the mean thermal optimum of the species recorded in the “past” and “recent” plots of each ecoregion. To this end, we calculated the weighted mean of the thermal optima of the species using their occurrence count in the ecoregion, independently of their local (plot scale) abundance. Then, thermophilization was obtained by subtracting the “recent” from the “past” occurrence-weighted means of the thermal optima. As our plots were not exactly separated by 10 years, we corrected the thermophilization rates by the average time difference of the plots to express thermophilization in degree Celsius *per* year ($^{\circ}\text{C yr}^{-1}$). This method of computing thermophilization differs from past studies using permanent plots, where changes in the mean thermal optimum are computed at the plot scale over time. Our approach did not investigate plot-scale changes (that were blurred by the semi-permanent nature of the pairs) but allowed studying the changes in the occurrence rates of species at the regional scale under homogenous environmental conditions.

We computed the individual contribution of each species to thermophilization (contrib_i), with the following formula:

$$\text{Contrib}_i = \frac{(Topt_i - Topt_{ecoreg\ past}) \cdot (occ_{i\ recent} - occ_{i\ past})}{\sum occ_{recent}} \quad (1)$$

Where $Topt_i$ is the thermal optimum of species i , $Topt_{ecoreg\ past}$ the weighted mean thermal optimum of the “past” occurrences, occ_i is the count of plots where the species was recorded in the “past” and “recent” periods, and $\sum occ_{recent}$ is the total number of occurrences of the “recent” period. Species with equal occurrences in the two periods resulted in a contrib_i of 0. Therefore, they did not contribute to the computation any further. The rationale behind this formula is that species thermal optima were assumed constant, and the number of “past” and “recent” plots were even, so that we did not expect any change in occurrences. Consequently, only changes in occurrences could alter the mean thermal optimum of an ecoregion. The term $(Topt_i - Topt_{ecoreg\ past})$ represents the extent to which an individual species deviated from the mean optima of the past period of the ecoregion. Thus it measures its relative adaptation to climate relative to every present species. It is then multiplied by $(occ_{i\ recent} - occ_{i\ past})$, the change in occurrences of the individual species, divided by $\sum occ_{recent}$ (this allows to scale contrib_i as the two periods will not have an equal number of total occurrences).

The sum of all $contrib_i$ results in the thermophilization value of a given ecoregion (see supplementary equations for a derivation of the equation). As a result, we partitioned the sums of $contrib_i$ into components that could be added to one another to obtain the thermophilization value. To create the extinction and colonization components, we added the $contrib_i$ of species with declining occurrences for extinction ($occ_{i\ recent} - occ_{i\ past} < 0$), and the $contrib_i$ of species with increasing occurrences for colonization ($occ_{i\ recent} - occ_{i\ past} > 0$). We subdivided these two components into the contributions of cold- and warm-adapted species to these components. The subcomponents depended on whether a species was locally cold-adapted ($Topt_i - Topt_{ecoreg\ past} < 0$) or warm-adapted ($Topt_i - Topt_{ecoreg\ past} > 0$) compared to the weighted mean thermal optimum of the ecoregion $Topt_{ecoreg\ past}$. The equation resulted in an easily interpretable $contrib_i$ term. For example, the contribution of the extinction of cold-adapted species [$(occ_{i\ recent} - occ_{i\ past} < 0) * (Topt_i - Topt_{ecoreg\ past} < 0)$] was always positive, i.e. it contributed to thermophilization. The contribution of extinction as a whole could either be positive or negative as it includes the extinction of both cold and warm-adapted species (eq (1)).

Computation and partitioning of beta-diversity changes

In parallel to the thermophilization analysis, we computed β -diversity using the Whittaker β_w metric (Whittaker, 1960) for each period. The Whittaker β_w was calculated as described in Eq (2):

$$\beta_w = \frac{\gamma}{\alpha} \quad (2)$$

Where γ is the total number of different species recorded in the ecoregion and α is the mean species richness of the plots present in the ecoregion. This metric is more suited to investigating differences between multiple communities than metrics using the means of pairwise differences because it accounts for species co-occurrences and measures heterogeneity by directly assessing the proportionality between local diversity and ecoregion diversity (Baselga, 2010; Socolar et al., 2016; Tatsumi et al., 2021). We did not use a metric relying on abundance because abundance is estimated based on a Braun-Blanquet scale in the NFI (Braun-blanquet, 1932) and is less reliable than presence/absence. Using abundance-based metrics can lead to both lower and higher estimates of β -diversity. Locally abundant ubiquitous species can lead to lower β -diversity estimates, whereas locally abundant species found in just a few plots lead to higher β -diversity estimates. Our study mostly documented the decline of cold-adapted species, whose local abundance was most probably low for these local extinctions to happen. Therefore, we did not expect underestimated homogenization following the decline of locally abundant cold-adapted

species. However, one caveat is that we cannot draw any conclusion on an increased abundance of warm-adapted species that could cause further homogenization and the removal of cold-adapted individuals.

We tested the assumption that different ecoregions displayed different species pools by comparing the β_w obtained in one ecoregion with the β_w obtained from the plots of the neighboring ecoregions. When β_w -diversity included several ecoregions, it increased 2-fold, demonstrating differences in the species pools of the ecoregions.

We computed β -diversity changes ($\Delta\beta$ -diversity) at the ecoregion level by subtracting the β_w of the “recent” plots from the β_w of the “past” plots. Then, we computed the contribution of each species to this change in β -diversity by adapting the methods and code presented in Tatsumi et al. (2021). This method assigns an extinction and colonization component to each species; however, we added these two components to obtain a unique value of contribution to $\Delta\beta$ -diversity *per* species. For example, a species can decrease β -diversity (homogenize) by declining if it was already rare, or by colonizing if it was an already widespread species. Conversely, colonization by a rare species or extinction of a widespread species have a positive impact on $\Delta\beta$ -diversity (heterogenization). We summed the contributions to $\Delta\beta$ -diversity following the same procedure as described in the previous section to obtain the contributions of declining species (extinction) and spreading species (colonization) to $\Delta\beta$ -diversity and know whether these species were locally cold- or warm-adapted, for a total of 4 components.

We tagged species as initially “rare” or “common” based on their baseline occupancy. Species occupying less than 10% of the “past” plots of an ecoregion were labeled as initially rare; if they occupied more than 10%, they were labeled as initially common. This simple classification matched the intuitive expectation of $\Delta\beta$ -diversity partitioning: extinction of rare species contributes to homogenization, while extinction of common species contributes to differentiation (see Tatsumi et al., 2021 - “Multiple-site variation” - for more information, Extended Fig.3). This classification accounts for species that may be common in one ecoregion but very infrequent or belong to unique communities in another. By design, this definition does not represent a classification of rarity, but rather the commonness of a species occurrences in a given ecoregion during the baseline period.

This common vs. rare species classification allowed testing other ecologically relevant processes possibly underlying an extinction or a colonization component. We further split the 4 contributions into “common” and “rare” species subcomponents, for a total of 8 contributions.

More cold-adapted than warm-adapted species were labeled “rare” across the ecoregions (Extended Fig.3). The lower baseline occupancy of rare cold-adapted species, rather than

their climate preference, could have been a confounding factor of extinction; that is, rare species might decline more rapidly, creating the pattern reported in the Results section (Fig.S1). We addressed this confounding factor by rarefying our dataset randomly so that the rare and common cold- and warm-adapted classification would display a balanced number of species and occurrences. Thus, observing the same pattern as the one reported in the main text indicates that increased chances of rare species extinction was not the sole explanation for our results (Table S4).

In order to have a comparable set of species and components to the set of the thermophilization analysis, the thermophilization and $\Delta\beta$ -diversity partitionings were done with the subset of species included in the thermal optimum database ClimPlant V1.2.

We ran the thermophilization and $\Delta\beta$ -diversity analyses and partitionings with the other two thermal optimum databases (Gégout et al., 2005) and found similar results and interpretations (Table S4).

Null models and bootstrapping

We created two null models to test whether changes in species occurrences were independent of the thermal optima, and to correct the analysis when the two periods had different numbers of occurrences.

To test the independence of changes in species occurrences relatively to their respective thermal optima, we ran 200 iterations of the above-described thermophilization analysis by randomizing the thermal optimum of species drawn from the species pool of each ecoregion. The 200 iterations of this analysis were averaged to create the null model. This null model (hereafter called random thermal optimum model) was used to test for differences with the partitioning results of the original dataset. We also tested each component of this model against 0 with a Wilcoxon test. The absence of significant thermophilization in the random thermal optimum model demonstrated a link between changes in species occurrences and their thermal optima (Extended Fig.1, Table S1).

The total number of occurrences recorded in our dataset decreased between the two periods although our sample had balanced numbers of “past” and “recent” plots. While this decrease may have been caused by true ecological factors such as climate-change-induced extinction, confounding methodological factors may also have been at play. In our dataset, more plots from the “past” period were surveyed during the growing season (53% in the “past” plots vs. 49% in the “recent” plot). During this period, species identification is easier, and more species are visible. To account for this potential bias, as well as to investigate $\Delta\beta$ -

diversity in a scenario where the average species richness remains unchanged, we conducted both the thermophilization and the β -diversity change analysis by equalizing the occurrence numbers between the historical and recent periods. More specifically, for each ecoregion, we randomly removed occurrences of the period with the greater number of total occurrences to match the total occurrences of the other period. We repeated this resampling and the analysis 200 times, (hereafter called the rarefaction null model). With this stricter methodology, thermophilization was still estimated at $0.012 \text{ }^\circ\text{C yr}^{-1}$ (s.d. 0.011), the extinction component at $0.010 \text{ }^\circ\text{C yr}^{-1}$ (s.d. 0.07), and the colonization component at $0.02 \text{ }^\circ\text{C yr}^{-1}$ (s.d. 0.08). The $\Delta\beta$ -diversity value, its extinction and colonization component were -0.31 (s.d. 1.5), -1.0 (s.d. 0.90), and 0.70 (s.d. 1.0), respectively (Table S2).

Statistical testing

We tested the significant difference from 0 (or the mean of the null model) of the mean of the seven components (global value, extinction, colonization, and the four subcomponents created with the relative thermal optima of the species) for the two metrics (thermophilization and $\Delta\beta$ -diversity) with the Wilcoxon signed-rank test (Rey & Neuhäuser, 2011). However, we chose a different reference for the test depending on the metrics and which hypothesis we were investigating. We tested the difference between the means of the thermophilization components and the means of the corresponding components of the random thermal optimum model. We tested the differences between the $\Delta\beta$ -diversity means with 0 as our null hypothesis (“no change in β -diversity”). Unlike thermophilization, the components were not constrained in their value (e.g. the contribution of colonizing warm-adapted species to thermophilization was strictly positive, 0 was not adequate for testing it, but its contribution to $\Delta\beta$ -diversity could be positive or negative).

For the sake of simplicity, we tested each component of thermophilization and $\Delta\beta$ -diversity only against 0 for the random thermal optimum model and the rarefaction null model.

We tested the significance and the magnitude of the correlation between thermophilization, $\Delta\beta$ -diversity and their two components (extinction and colonization) with mean annual temperature using linear regressions. The applicability of linear regressions was checked through normality and homoscedasticity of the residuals and the independence to confounding variables, following the recommendation of Zuur et al. (2010).

We conducted our analyses in R 4.2.2 statistical environment (R Core Team, 2019), with the ‘data.table’ (Dowle & Srinivasan, 2020), ‘ggplot2’ (Wickham, 2011), ‘sf’ (Pebesma, 2018), ‘ggpubr’ (Kassambara, 2023), ‘foreach’ (Microsoft & Weston, 2022) ‘ggspatial’ (Dunnington & Thorne, 2020; OpenStreetMap contributors, 2017), and ‘doParallel’ (Corporation &

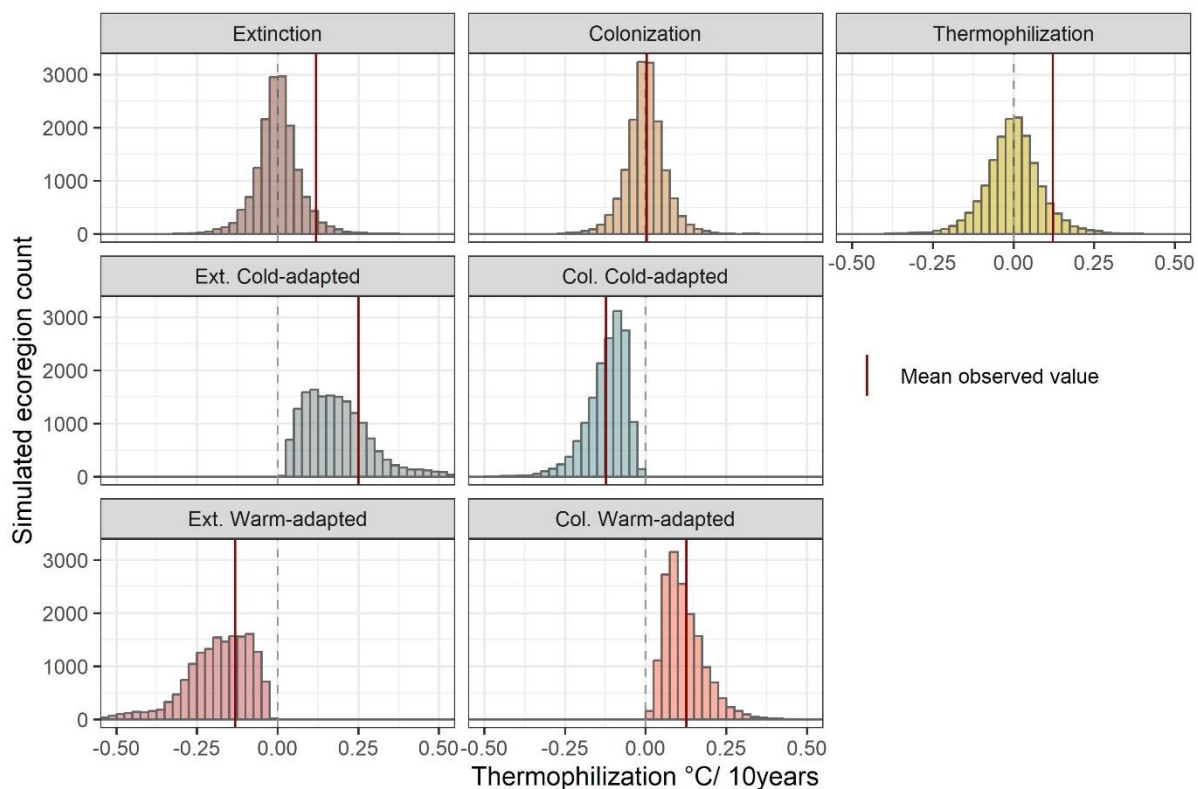
Weston, 2022) packages. We were inspired by the ‘ecopart’ method and adapted the code presented by Tatsumi et al. (2021) for $\Delta\beta$ -diversity partitioning.

Data availability

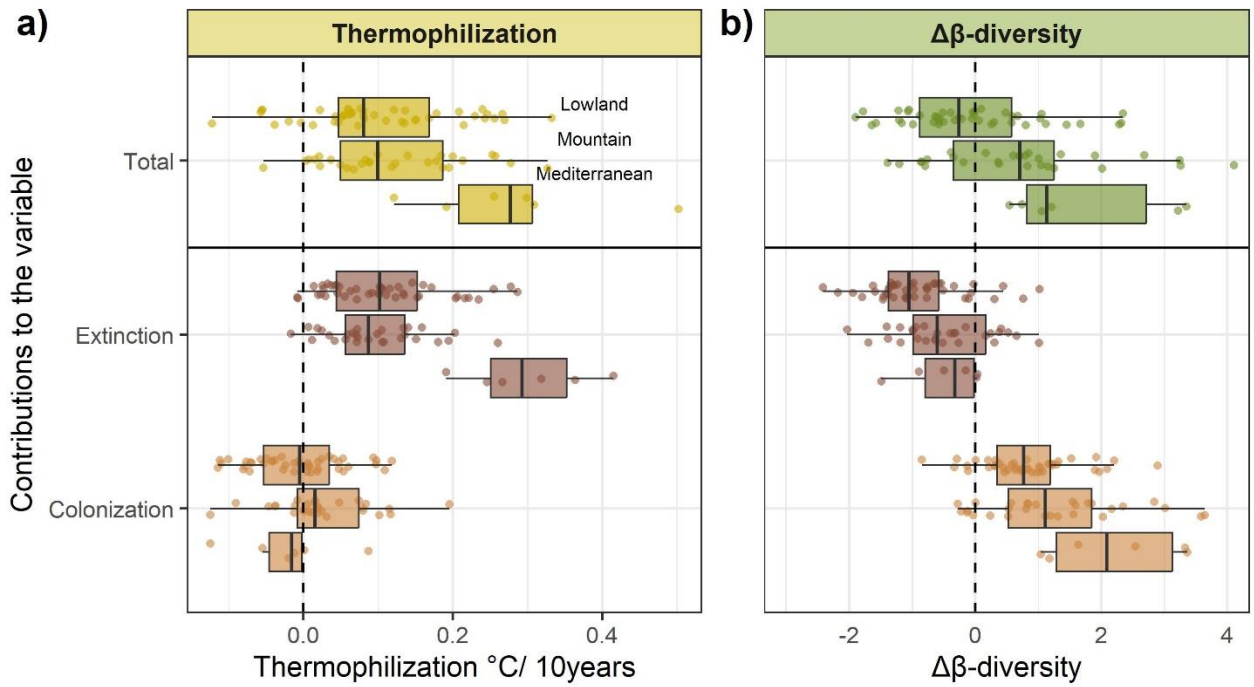
French National Forest Inventory data are freely distributed by the French Institute for Geographic and Forest Information (IGN) at <https://inventaire-forestier.ign.fr>

The dataset and the code used to reproduce our analysis can be downloaded from GitHub https://github.com/Jeremy-borderieux/Article_thermo_beta_part.git.

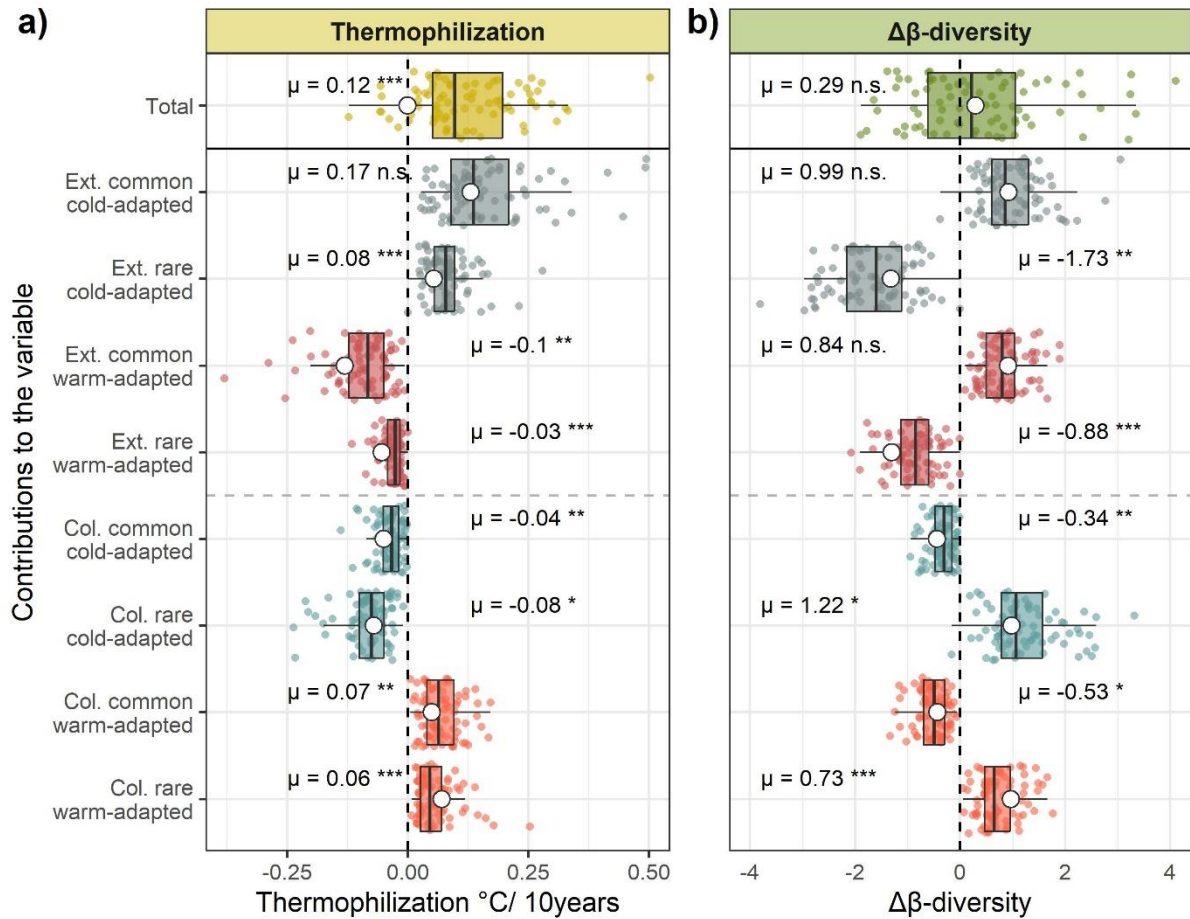
4. Extended Figures



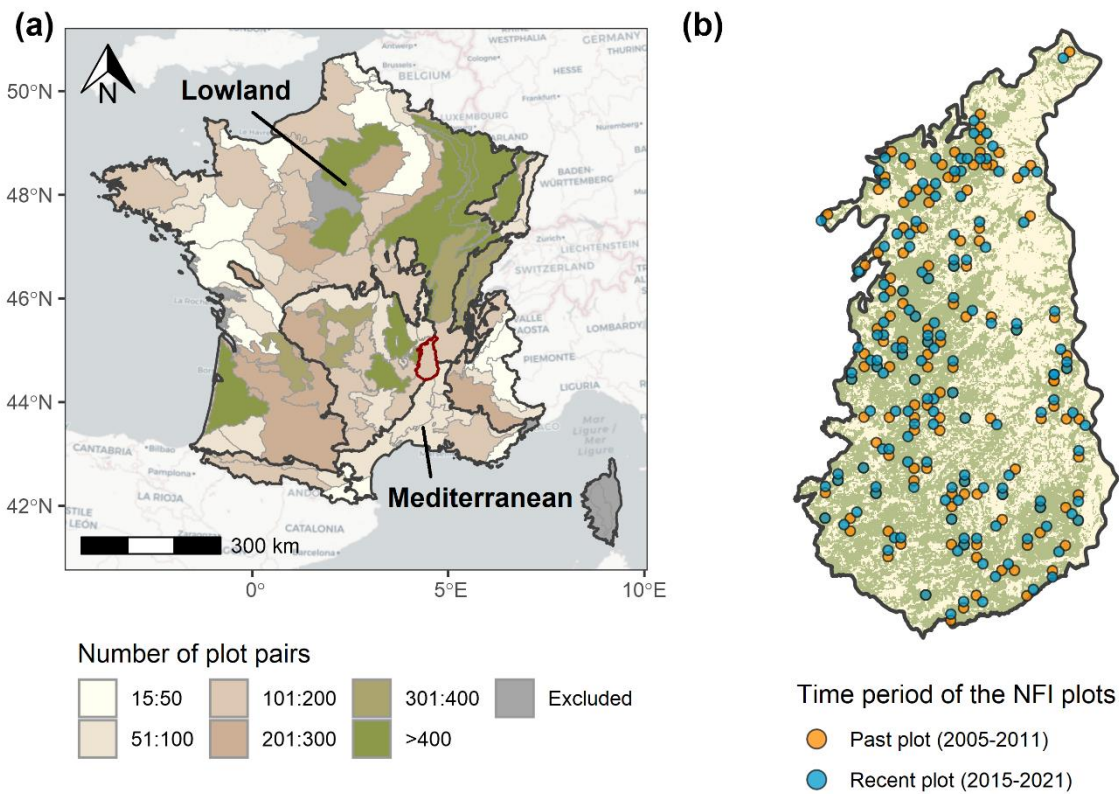
Extended Figure 1: Results of the 200 iterations of the random thermal optimum model (thermal optima randomly assigned to the species). In this figure, the runs are not averaged: the 80 ecoregions randomized 200 times are displayed. The average values of thermophilization, $\Delta\beta$ -diversity and their contribution of the original dataset are displayed.



Extended Figure 2: Thermophilization and $\Delta\beta$ -diversity in lowland, mountain and Mediterranean ecoregion clusters (Extended Fig.1). Lowland (8,271 pairs, 45 ecoregions), mountain (4,116 pairs, 29 ecoregions), Mediterranean (377 pairs, 6 ecoregions). Each dot represents the values of one of the 80 ecoregions ($n_{tot}=80$).



Extended Figure 3: Partitioning of the data presented in Fig.3. The contributions to a) thermophilization ($^{\circ}\text{C decade}^{-1}$), and b) $\Delta\beta$ -diversity (unitless) were partitioned on the basis of species declining or increasing in occurrences, of their thermal optimum relative to their ecoregion, and whether these species were rare (baseline occurrences <10% of the plots) or common (baseline occurrences >10% of the plots). Each dot represents the values of one of the 80 ecoregions ($n_{\text{tot}}=80$). The dashed gray line delineates the colonization and extinction components. The mean of each component is displayed. White dot; mean value of the thermophilization null model. The statistical difference between the null model value and the original dataset, obtained with a two-sided Wilcoxon test, is also displayed: $p<0.05$ (*), $p<0.01$ (**), $p<0.001$ (***). Exact P-values are available in Table S1. Boxes; 25th centile, median and 75th centile; whiskers, 1.5 times the interquartile range.



Extended Figure 4: (a) Map of the 86 forest ecoregions of France, with a colored gradient representing the number of plot pairs. Three main biomes (lowland, Mediterranean, mountain) cluster different ecoregions delineated with bold black lines. The clusters without a label are mountain ecoregions. The zoomed ecoregion in (b) is outlined in red in (a). (b) Example of the plot pair sampling design, with NFI plot localization. Some plots may overlap. Green, forested areas. Basemap credits: (OpenStreetMap contributors, 2017)

5. Supplementary materials

Table S1: Thermophilization ($^{\circ}\text{C}/\text{decades}^{-1}$) and $\Delta\beta$ -diversity and their component mean value (Value) and standard deviation (s.d) across 80 forest ecoregions. The value from the original dataset (14,167 pairs of plots) and the randomized thermal optimum null model (see methods) are displayed. The P-value were obtained with a two-sided Wilcoxon one sample test against 0.

Variable	Original dataset			Null thermophilization model		
	Value	s.d	P-value	Value	s.d	P-value
Thermophilization	0,122	0,11	1,53e-12	-4,13e-04	0,0054	0,589
Extinction	0,118	0,089	1,21e-14	-2,05e-04	0,0047	0,315
Colonization	0,00346	0,065	0,664	-2,08e-04	0,0037	0,516
Cold-adapted extinction	0,25	0,14	8,00e-15	0,185	0,096	8,00e-15
Cold-adapted colonization	-0,132	0,087	8,00e-15	-0,186	0,096	8,00e-15
Warm-adapted extinction	-0,123	0,061	8,00e-15	-0,122	0,055	8,00e-15
Warm-adapted colonization	0,126	0,061	8,00e-15	0,121	0,055	8,00e-15
$\Delta\beta$ -diversity	0,291	1,4	0,107	0,291	1,4	0,107
Extinction	-0,785	0,91	1,93e-10	-0,785	0,91	1,93e-10
Colonization	1,08	0,97	5,55e-13	1,08	0,97	5,55e-13
Cold-adapted extinction	-0,744	0,82	5,22e-12	-0,396	0,48	1,81e-10
Cold-adapted colonization	-0,0417	0,46	0,397	-0,39	0,44	1,75e-10
Warm-adapted extinction	0,877	0,72	6,92e-14	0,542	0,49	5,35e-13
Warm-adapted colonization	0,199	0,45	0,000159	0,534	0,49	5,35e-13

Table S2: Thermophilization ($^{\circ}\text{C}/\text{decades}^{-1}$) and $\Delta\beta$ -diversity and their component mean value (Value) and standard deviation (s.d) across 80 forest ecoregions. The value from the original dataset (14,167 pairs of plots) and the randomized original dataset where occurrences are rarefied so that each time period have an equal number of occurrences. The P-value were obtained with a two-sided Wilcoxon one sample test against 0.

Variable	Original dataset			Rarefaction null model		
	Value	s.d	P-value	Value	s.d	P-value
Thermophilization	0,122	0,11	1,53e-12	0,121	0,011	1,47e-12
Extinction	0,118	0,089	1,21e-14	0,104	0,0071	1,46e-14
Colonization	0,00346	0,065	0,664	0,0167	0,0072	0,049
Cold-adapted extinction	0,25	0,14	8,00e-15	0,205	0,0085	8,00e-15
Cold-adapted colonization	-0,132	0,087	8,00e-15	-0,101	0,0053	8,00e-15
Warm-adapted extinction	-0,123	0,061	8,00e-15	-0,144	0,006	8,00e-15
Warm-adapted colonization	0,126	0,061	8,00e-15	0,161	0,007	8,00e-15
$\Delta\beta$ -diversity	0,291	1,4	0,107	-0,314	1,5	0,0855
Extinction	-0,785	0,91	1,93e-10	-1,01	0,9	3,38e-13
Colonization	1,08	0,97	5,55e-13	0,696	1	2,76e-07
Cold-adapted extinction	-0,744	0,82	5,22e-12	-0,825	0,77	9,96e-14
Cold-adapted colonization	-0,0417	0,46	0,397	-0,185	0,4	0,000141
Warm-adapted extinction	0,877	0,72	6,92e-14	0,771	0,75	3,98e-12
Warm-adapted colonization	0,199	0,45	0,000159	-0,0752	0,55	0,253

Table S3: Thermophilization ($^{\circ}\text{C}/\text{decades}^{-1}$) and $\Delta\beta$ -diversity and their component mean value (Value) and standard deviation (s.d) across 80 forest ecoregions. The analysis was performed with two other thermal optimum value, from the original 2005 and a 2019 analysis of the EcoPlant database¹. The P-value were obtained with a two-sided Wilcoxon one sample test against 0.

Variable	EcoPlant Thermal optimum 2005			EcoPlant thermal optimum 2019		
	Value	s.d	P-value	Value	s.d	P-value
Thermophilization	0,111	0,15	9,63e-11	0,061	0,2	0,0038
Extinction	0,0965	0,085	8,61e-14	0,072	0,12	8,11e-08
Colonization	0,0147	0,11	0,11	-0,011	0,15	0,212
Cold-adapted extinction	0,273	0,16	8,00e-15	0,31	0,18	8,00e-15
Cold-adapted colonization	-0,177	0,12	8,00e-15	-0,238	0,18	8,00e-15
Warm-adapted extinction	-0,165	0,09	8,00e-15	-0,208	0,12	8,00e-15
Warm-adapted colonization	0,18	0,11	8,00e-15	0,197	0,16	8,00e-15
$\Delta\beta$ -diversity	0,0511	1,2	0,941	0,0401	1,1	0,772
Extinction	-0,715	0,74	8,22e-11	-0,136	0,61	0,012
Colonization	0,766	0,83	1,25e-11	0,176	0,68	0,0422
Cold-adapted extinction	-0,628	0,68	2,39e-12	-0,307	0,49	9,15e-07
Cold-adapted colonization	-0,0868	0,47	0,0709	0,172	0,43	0,00206
Warm-adapted extinction	0,578	0,55	2,56e-12	0,24	0,48	6,93e-05
Warm-adapted colonization	0,188	0,48	0,00178	-0,0637	0,37	0,166

Table S4: Thermophilization ($^{\circ}\text{C}/\text{decades}^{-1}$) and $\Delta\beta$ -diversity and their component mean value (Value) and standard deviation (s.d) across 80 forest ecoregions. The value from the original dataset (14,167 pairs of plots) is displayed. The value from subsets of the dataset created by balancing the number of “rare” species within the cold and warm-adapted categories (and to a lesser extend “common”) is also displayed. The P-value were obtained with a two-sided Wilcoxon one sample test against 0.

Variable	Original dataset			Even “rare” species null model		
	Value	s.d	P-value	Value	s.d	P-value
Thermophilization	0,122	0,11	1,53e-12	0,133	0,11	6,43e-14
Extinction	0,118	0,089	1,21e-14	0,102	0,084	2,05e-14
Colonization	0,00346	0,065	0,664	0,0319	0,059	5,90e-06
Cold-adapted extinction	0,25	0,14	8,00e-15	0,233	0,14	8,00e-15
Cold-adapted colonization	-0,132	0,087	8,00e-15	-0,131	0,091	8,00e-15
Warm-adapted extinction	-0,123	0,061	8,00e-15	-0,0975	0,051	8,00e-15
Warm-adapted colonization	0,126	0,061	8,00e-15	0,129	0,067	8,00e-15
$\Delta\beta$ -diversity	0,291	1,4	0,107	0,391	1,2	0,0064
Extinction	-0,785	0,91	1,93e-10	-0,48	0,8	6,33e-07
Colonization	1,08	0,97	5,55e-13	0,871	0,84	1,20e-12
Cold-adapted extinction	-0,744	0,82	5,22e-12	-0,287	0,57	2,28e-06
Cold-adapted colonization	-0,0417	0,46	0,397	-0,193	0,44	0,000175
Warm-adapted extinction	0,877	0,72	6,92e-14	0,544	0,48	3,63e-13
Warm-adapted colonization	0,199	0,45	0,000159	0,327	0,49	5,15e-08

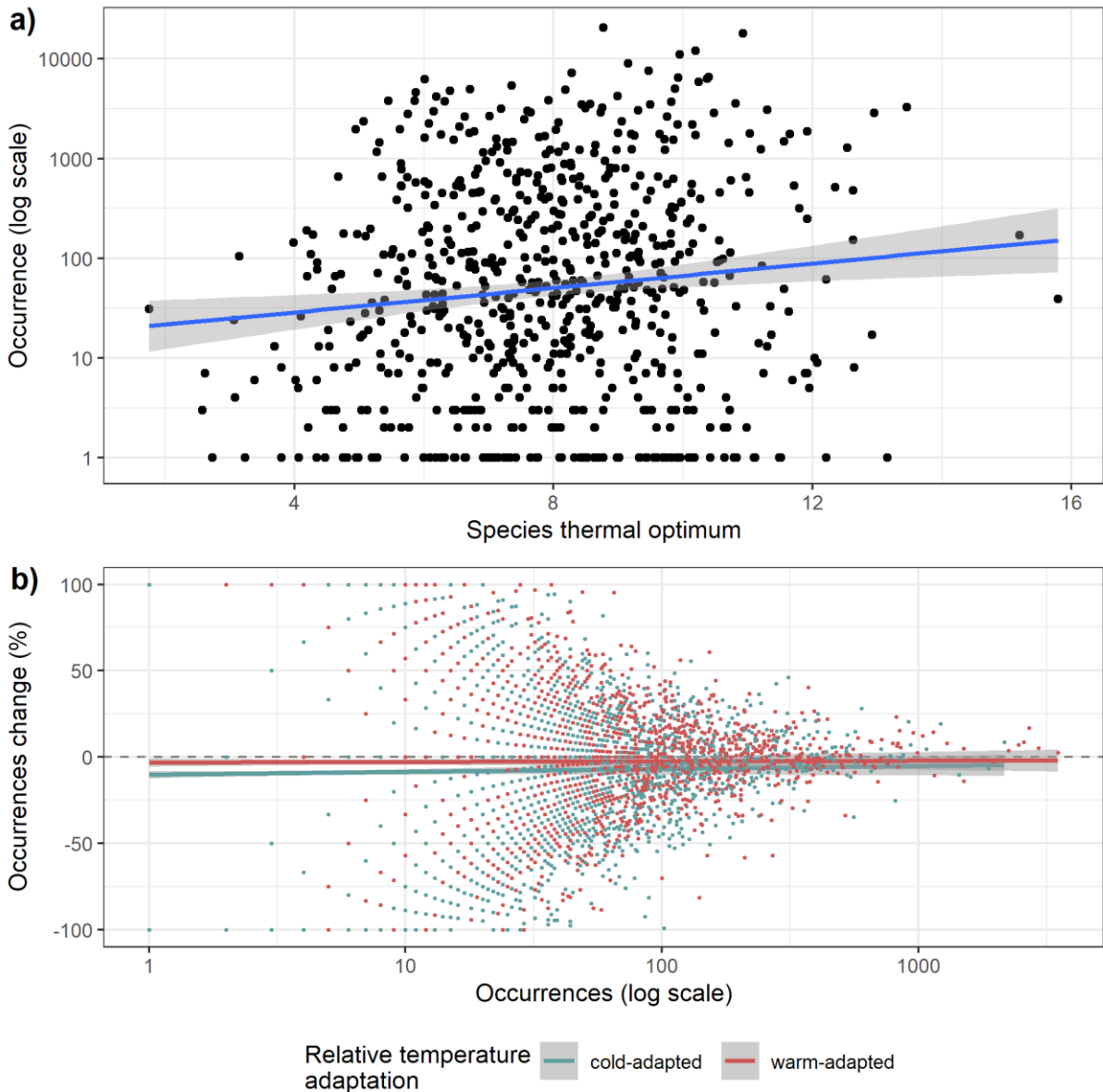


Figure S1: a) Species occurrences (presence in a plot, log scale) in the entire dataset ($n=28,334$ plots) in relation to their thermal optimum. The blue line is a fitted linear model $\log(\text{occurrences}) \sim \text{thermal optimum}$ and its uncertainty (error bar, confidence interval). b) Y-axis: Relative change in occurrences in each ecoregion for each species. (0% mean stable occurrences, 100% a species whose occurrences are only found in the “recent” period of the ecoregion, - 100% a species that lost every occurrence between the two periods, 50% and -50 an increase or decrease, respectively, of 50% the “past” occurrences). X-axis: total occurrence (log scale). The species and the linear fit $\text{Proportion} \sim \log(\text{occurrences})$ are separated based on whether they were classified as locally cold or warm-adapted species in the given ecoregion. The error band around the model is the confidence interval of the linear model.

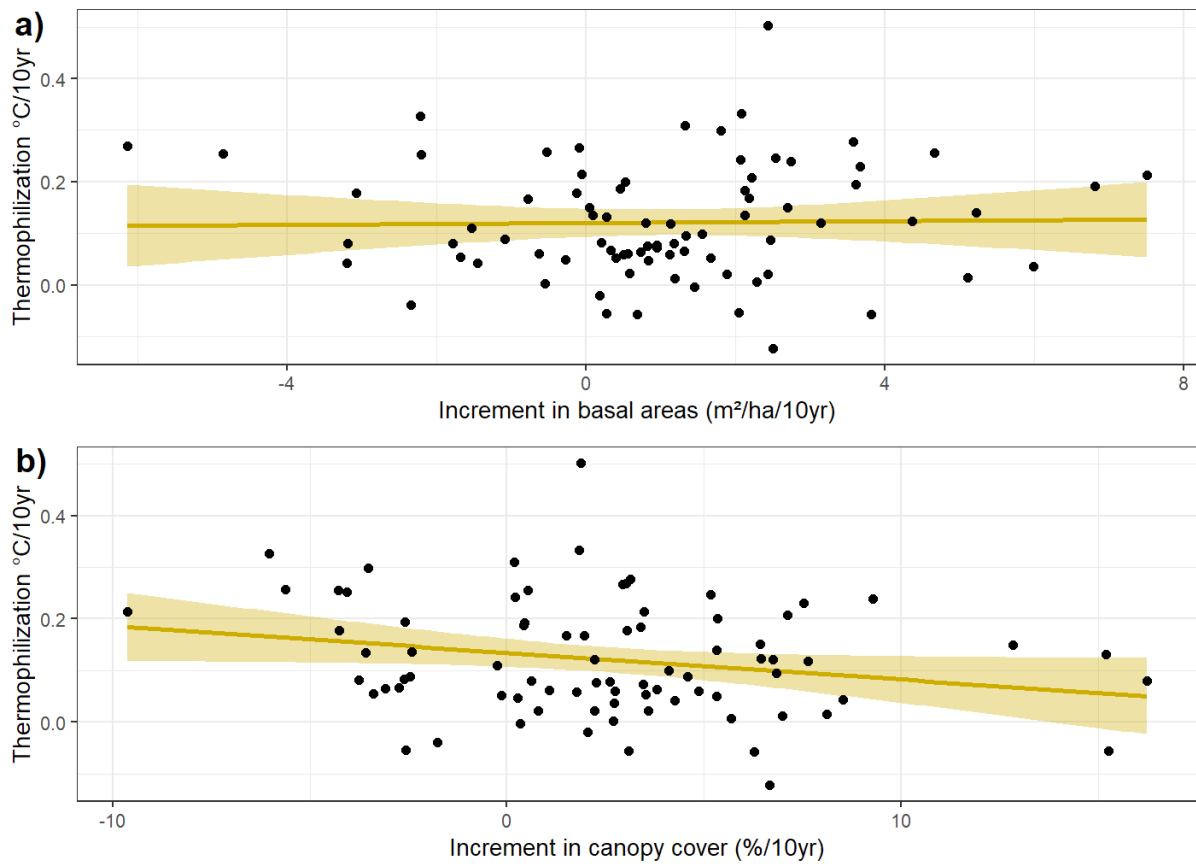


Figure S2: Thermophilization of the 80 ecoregions as a function of the increment of their mean basal area (a) and canopy cover (b). The increments are computed as a difference of the mean value of basal area or canopy cover between the “recent” and the “past” plots, a positive value means an increase. A linear model and its uncertainty is displayed, the R^2 of 5.0% of (b) is significantly different from 0. The error band around the model is the confidence interval of the linear model.

Supplementary equations.

We define the weighted thermal optimum of an ecoregion of the past period as follow:

$$Topt_{eco\ past} = \frac{\sum_i Topt_i * occ_{i\ past}}{\sum occ_{past}} \quad (1)$$

Where $Topt_i$ and $occ_{i\ past}$ are the thermal optimum and occurrences in the “past” period of the species i , respectively.

$\sum occ_{past}$ is the sum of past occurrences of every species, can also be written $\sum_i occ_{i\ past}$.

We define the weighted thermal optimum of an ecoregion of the recent period as follow:

$$Topt_{eco\ recent} = \frac{\sum_i Topt_i * occ_{i\ recent}}{\sum occ_{recent}} \quad (2)$$

Where $occ_{i\ recent}$ is the occurrences of the species i in the “recent” period.

Thus, thermophilization is defined as follow:

$$Thermophilization = Topt_{eco\ recent} - Topt_{eco\ past} \quad (3)$$

We defined the species i contribution to thermophilization with the equation:

$$Contrib_i = \frac{(Topt_i - Topt_{eco\ past}) \cdot (occ_{i\ recent} - occ_{i\ past})}{\sum occ_{recent}} \quad (4)$$

And we want to demonstrate that

$$\sum_i contrib_i = Thermophilization \quad (5)$$

We first develop (4)

$$Contrib_i =$$

$$\frac{Topt_i * occ_{i\ recent} - Topt_{eco\ past} * occ_{i\ recent} + Topt_{eco\ past} * occ_{i\ past} - Topt_i * occ_{i\ past}}{\sum occ_{recent}} \quad (6)$$

Then the sum of (6) is written as follow:

$$\sum_i contrib_i =$$

$$\frac{\sum_i Topt_i * occ_{i\ recent} - Topt_{eco\ past} * \sum_i occ_{i\ recent} + Topt_{eco\ past} * \sum_i occ_{i\ past} - \sum_i Topt_i * occ_{i\ past}}{\sum occ_{recent}} \quad (7)$$

We can then simply (7) to

$$\sum_i contrib_i = \frac{\sum_i Topt_i * occ_{i\ recent}}{\sum occ_{recent}} - \frac{Topt_{eco\ past} * \sum_i occ_{i\ recent}}{\sum occ_{recent}} + \frac{Topt_{eco\ past} * \sum_i occ_{i\ past} - \sum_i Topt_i * occ_{i\ past}}{\sum occ_{recent}} \quad (8)$$

We can further simplify (8) to

$$\sum_i contrib_i = Topt_{eco\ recent} - Topt_{eco\ past} + \Phi \quad (9)$$

With:

$$\Phi = \frac{Topt_{eco\ past} * \sum_i occ_{i\ past} - \sum_i Topt_i * occ_{i\ past}}{\sum occ_{recent}} \quad (10)$$

We thus need to prove that $\Phi = 0$, however:

$$Topt_{eco\ past} * \sum_i occ_{i\ past} = \sum_i Topt_i * occ_{i\ past} \quad (11)$$

Thus:

$$\Phi = \frac{\sum_i Topt_i * occ_{i\ past} - \sum_i Topt_i * occ_{i\ past}}{\sum occ_{recent}} = 0 \quad (12)$$

Which leads to

$$\sum_i contrib_i = Topt_{eco\ recent} - Topt_{eco\ past} = Thermophilization \quad (13)$$

6. Acknowledgments

The authors are grateful to the French institute for geographic and forest information (IGN) and their field technicians for providing the NFI data and a precise description of the forest ecoregions. The authors are grateful to the 3 reviewers whose comments greatly improved the manuscript. The authors acknowledge the funding from the Labex Arbre. JB was funded by a joint AgroParisTech and Région Grand- Est grant (grant number 19_GE8_01020p05035) and JMSD was funded by the ANR-JCJC (Agence Nationale de la Recherche, jeunes chercheuses et jeunes chercheurs) SEEDFOR (ANR-21-CE32-0003). JMSD acknowledges the support from NASA for UConn's Ecological Modeling Institute (#80NSSC 22K0883).

7. Author contribution statement

Conceptualization: JB, JCG & JSMD. Analysis, visualization, methodology and software: JB. Supervision and funding acquisition: JCG & JSMD. JB wrote the manuscript with contributions from all co-authors.

8. References

- Baeten, L., Vangansbeke, P., Hermy, M., Peterken, G., Vanhuyse, K., & Verheyen, K. (2012). Distinguishing between turnover and nestedness in the quantification of biotic homogenization. *Biodiversity and Conservation*, 21(6), 1399-1409. <https://doi.org/10.1007/s10531-012-0251-0>
- Bahn, M., & Körner, Ch. (2003). Recent Increases in Summit Flora Caused by Warming in the Alps. In L. Nagy, G. Grabherr, C. Körner, & D. B. A. Thompson (Eds.), *Alpine Biodiversity in Europe* (pp. 437-441). Springer. https://doi.org/10.1007/978-3-642-18967-8_27
- Baselga, A. (2010). Partitioning the turnover and nestedness components of beta diversity: Partitioning beta diversity. *Global Ecology and Biogeography*, 19(1), 134-143. <https://doi.org/10.1111/j.1466-8238.2009.00490.x>
- Bergès, L., Pellissier, V., Avon, C., Verheyen, K., & Dupouey, J.-L. (2013). Unexpected long-range edge-to-forest interior environmental gradients. *Landscape Ecology*, 28(3), 439-453. <https://doi.org/10.1007/s10980-012-9841-1>
- Bertrand, R., Lenoir, J., Piedallu, C., Riofrío-Dillon, G., de Ruffray, P., Vidal, C., Pierrat, J.-C., & Gégout, J.-C. (2011). Changes in plant community composition lag behind climate warming in lowland forests. *Nature*, 479(7374), 517-520. <https://doi.org/10.1038/nature10548>
- Bertrand, R., Riofrío-Dillon, G., Lenoir, J., Drapier, J., de Ruffray, P., Gégout, J.-C., & Loreau, M. (2016). Ecological constraints increase the climatic debt in forests. *Nature Communications*, 7(1), 12643. <https://doi.org/10.1038/ncomms12643>

- Bodin, J., Badeau, V., Bruno, E., Cluzeau, C., Moisselin, J.-M., Walther, G.-R., & Dupouey, J.-L. (2013). Shifts of forest species along an elevational gradient in Southeast France: Climate change or stand maturation? *Journal of Vegetation Science*, 24(2), 269-283. <https://doi.org/10.1111/j.1654-1103.2012.01456.x>
- Boulangeat, I., Gravel, D., & Thuiller, W. (2012). Accounting for dispersal and biotic interactions to disentangle the drivers of species distributions and their abundances: The role of dispersal and biotic interactions in explaining species distributions and abundances. *Ecology Letters*, 15(6), 584-593. <https://doi.org/10.1111/j.1461-0248.2012.01772.x>
- Braun-blanquet, J. (1932). Plant sociology. The study of plant communities. First ed. *Plant Sociology. The Study of Plant Communities. First Ed.* <https://www.cabdirect.org/cabdirect/abstract/19331600801>
- Cholewińska, O., Adamowski, W., & Jaroszewicz, B. (2020). Homogenization of Temperate Mixed Deciduous Forests in Białowieża Forest: Similar Communities Are Becoming More Similar. *Forests*, 11(5), 545. <https://doi.org/10.3390/f11050545>
- Chytrý, M., Tichý, L., Hennekens, S. M., & Schaminée, J. H. J. (2014). Assessing vegetation change using vegetation-plot databases: A risky business. *Applied Vegetation Science*, 17(1), 32-41. <https://doi.org/10.1111/avsc.12050>
- Corporation, M., & Weston, S. (2022). *doParallel: Foreach Parallel Adaptor for the "parallel" Package*. <https://CRAN.R-project.org/package=doParallel>
- Crisfield, V., Blanchet, F. G., Raudsepp-Hearne, C., & Gravel, D. (2023). *How and why species are rare: Towards an understanding of the ecological causes of rarity* [Preprint]. Preprints. <https://doi.org/10.22541/au.169107484.46077531/v1>
- Danneyrolles, V., Vellend, M., Dupuis, S., Boucher, Y., Laflamme, J., Bergeron, Y., Fortin, G., Leroyer, M., de Römer, A., Terrail, R., & Arseneault, D. (2021). Scale-dependent changes in tree diversity over more than a century in eastern Canada: Landscape diversification and regional homogenization. *Journal of Ecology*, 109(1), 273-283. <https://doi.org/10.1111/1365-2745.13474>
- De Frenne, P., Rodríguez-Sánchez, F., Coomes, D. A., Baeten, L., Verstraeten, G., Vellend, M., Bernhardt-Romermann, M., Brown, C. D., Brunet, J., Cornelis, J., Decocq, G. M., Dierschke, H., Eriksson, O., Gilliam, F. S., Hedl, R., Heinken, T., Hermy, M., Hommel, P., Jenkins, M. A., ... Verheyen, K. (2013). Microclimate moderates plant responses to macroclimate warming. *Proceedings of the National Academy of Sciences*, 110(46), 18561-18565. <https://doi.org/10.1073/pnas.1311190110>
- De Frenne, P., Rodríguez-Sánchez, F., De Schrijver, A., Coomes, D. A., Hermy, M., Vangansbeke, P., & Verheyen, K. (2015). Light accelerates plant responses to warming. *Nature Plants*, 1(9), 1-3. <https://doi.org/10.1038/nplants.2015.110>
- De Frenne, P., Zellweger, F., Rodríguez-Sánchez, F., Scheffers, B. R., Hylander, K., Luoto, M., Vellend, M., Verheyen, K., & Lenoir, J. (2019). Global buffering of temperatures under forest canopies. *Nature Ecology & Evolution*, 3(5), 744-749. <https://doi.org/10.1038/s41559-019-0842-1>

- De Lombaerde, E., Vangansbeke, P., Lenoir, J., Van Meerbeek, K., Lembrechts, J., Rodríguez-Sánchez, F., Luoto, M., Scheffers, B., Haesen, S., Aalto, J., Christiansen, D. M., De Pauw, K., Depauw, L., Govaert, S., Greiser, C., Hampe, A., Hylander, K., Klinges, D., Koelemeijer, I., ... De Frenne, P. (2021). Maintaining forest cover to enhance temperature buffering under future climate change. *Science of The Total Environment*, 151338. <https://doi.org/10.1016/j.scitotenv.2021.151338>
- Devictor, V., van Swaay, C., Brereton, T., Brotons, L., Chamberlain, D., Heliölä, J., Herrando, S., Julliard, R., Kuussaari, M., Lindström, Å., Reif, J., Roy, D. B., Schweiger, O., Settele, J., Stefanescu, C., Van Strien, A., Van Turnhout, C., Vermouzek, Z., WallisDeVries, M., ... Jiguet, F. (2012). Differences in the climatic debts of birds and butterflies at a continental scale. *Nature Climate Change*, 2(2), 121-124. <https://doi.org/10.1038/nclimate1347>
- Dietz, L., Collet, C., Dupouey, J.-L., Lacombe, E., Laurent, L., & Gégout, J.-C. (2020). Windstorm-induced canopy openings accelerate temperate forest adaptation to global warming. *Global Ecology and Biogeography*. <https://doi.org/10.1111/geb.13177>
- Dowle, M., & Srinivasan, A. (2020). *data.table: Extension of `data.frame`*. <https://CRAN.R-project.org/package=data.table>
- Dullinger, S., Gattringer, A., Thuiller, W., Moser, D., Zimmermann, N. E., Guisan, A., Willner, W., Plutzer, C., Leitner, M., Mang, T., Caccianiga, M., Dirnböck, T., Ertl, S., Fischer, A., Lenoir, J., Svenning, J.-C., Psomas, A., Schmatz, D. R., Silc, U., ... Hülber, K. (2012). Extinction debt of high-mountain plants under twenty-first-century climate change. *Nature Climate Change*, 2(8), Article 8. <https://doi.org/10.1038/nclimate1514>
- Dunnington, D., & Thorne, B. (2020). *ggspatial: Spatial Data Framework for ggplot2. R Package Version 1, 1*.
- Dupouey, J.-L., Sciama, D., Dambrine, E., Rameau, J.-C., & Koerner, W. (2002). La Végétation des forêts anciennes. *Revue Forestière Française*, 6, 521. <https://doi.org/10.4267/2042/4940>
- Engler, R., Randin, C. F., Thuiller, W., Dullinger, S., Zimmermann, N. E., Araújo, M. B., Pearman, P. B., Le Lay, G., Piedallu, C., Albert, C. H., Choler, P., Coldea, G., De LAMO, X., Dirnböck, T., Gégout, J.-C., Gómez-García, D., Grytnes, J.-A., Heegaard, E., Høistad, F., ... Guisan, A. (2011). 21st century climate change threatens mountain flora unequally across Europe: CLIMATE CHANGE IMPACTS ON MOUNTAIN FLORAE. *Global Change Biology*, 17(7), 2330-2341. <https://doi.org/10.1111/j.1365-2486.2010.02393.x>
- Fischer, A., Lindner, M., Abs, C., & Lasch, P. (2002). Vegetation dynamics in central european forest ecosystems (near-natural as well as managed) after storm events. *Folia Geobotanica*, 37(1), 17-32. <https://doi.org/10.1007/BF02803188>
- Franklin, J., Serra-Diaz, J. M., Syphard, A. D., & Regan, H. M. (2016). Global change and terrestrial plant community dynamics. *Proceedings of the National Academy of Sciences*, 113(14), 3725-3734. <https://doi.org/10.1073/pnas.1519911113>

- Franks, S. J., Weber, J. J., & Aitken, S. N. (2014). Evolutionary and plastic responses to climate change in terrestrial plant populations. *Evolutionary Applications*, 7(1), 123-139. <https://doi.org/10.1111/eva.12112>
- Gargominy, O. (2022). *TAXREF v13.0, référentiel taxonomique pour la France*. [dataset]. UMS PatriNat (OFB-CNRS-MNHN), Paris. <https://doi.org/10.15468/VQUEAM>
- Gasperini, C., Carrari, E., Govaert, S., Meeussen, C., De Pauw, K., Plue, J., Sanczuk, P., Vanneste, T., Vangansbeke, P., Jacopetti, G., De Frenne, P., & Selvi, F. (2021). Edge effects on the realised soil seed bank along microclimatic gradients in temperate European forests. *Science of The Total Environment*, 798, 149373. <https://doi.org/10.1016/j.scitotenv.2021.149373>
- Gégout, J.-C., Coudun, C., Bailly, G., & Jabiol, B. (2005). EcoPlant: A forest site database linking floristic data with soil and climate variables. *Journal of Vegetation Science*, 16(2), 257-260. <https://doi.org/10.1111/j.1654-1103.2005.tb02363.x>
- Gosselin, F. (2016). Putting floristic thermophilization in forests into a conservation biology perspective: Beyond mean trait approaches. *Annals of Forest Science*, 73(2), Article 2. <https://doi.org/10.1007/s13595-015-0526-1>
- Gottfried, M., Pauli, H., Futschik, A., Akhalkatsi, M., Barančok, P., Benito Alonso, J. L., Coldea, G., Dick, J., Erschbamer, B., Fernández Calzado, M. R., Kazakis, G., Krajčič, J., Larsson, P., Mallaun, M., Michelsen, O., Moiseev, D., Moiseev, P., Molau, U., Merzouki, A., ... Grabherr, G. (2012). Continent-wide response of mountain vegetation to climate change. *Nature Climate Change*, 2(2), Article 2. <https://doi.org/10.1038/nclimate1329>
- Govaert, S., Vangansbeke, P., Blondeel, H., Steppe, K., Verheyen, K., & De Frenne, P. (2021). Rapid thermophilization of understorey plant communities in a 9 year-long temperate forest experiment. *Journal of Ecology*. <https://doi.org/10.1111/1365-2745.13653>
- Heinrichs, S., & Schmidt, W. (2017). Biotic homogenization of herb layer composition between two contrasting beech forest communities on limestone over 50 years. *Applied Vegetation Science*, 20(2), 271-281. <https://doi.org/10.1111/avsc.12255>
- IGN. (2013). *Fiches descriptives des grandes régions écologiques (GRECO) et des sylvoécorégions (SER)*. <https://inventaire-forestier.ign.fr/spip.php?article773>
- IGN. (2019, December 1). Le mémento de l'inventaire forestier. *Institut National de l'Information Géographique et Forestière*. <http://www.ign.fr/institut/publications/memento-linventaire-forestier>
- Jackson, S. T., & Sax, D. F. (2010). Balancing biodiversity in a changing environment: Extinction debt, immigration credit and species turnover. *Trends in Ecology & Evolution*, 25(3), 153-160. <https://doi.org/10.1016/j.tree.2009.10.001>
- Kassambara, A. (2023). *ggpubr: "ggplot2" Based Publication Ready Plots*. <https://CRAN.R-project.org/package=ggpubr>
- Kubisch, A., Degen, T., Hovestadt, T., & Poethke, H. J. (2013). Predicting range shifts under global change: The balance between local adaptation and dispersal. *Ecography*, 36(8), 873-882. <https://doi.org/10.1111/j.1600-0587.2012.00062.x>

- Kuhn, E., & Gégout, J. (2019). Highlighting declines of cold-demanding plant species in lowlands under climate warming. *Ecography*, 42(1), 36-44. <https://doi.org/10.1111/ecog.03469>
- Landuyt, D., De Lombaerde, E., Perring, M. P., Hertzog, L. R., Ampoorter, E., Maes, S. L., De Frenne, P., Ma, S., Proesmans, W., Blondeel, H., Sercu, B. K., Wang, B., Wasof, S., & Verheyen, K. (2019). The functional role of temperate forest understorey vegetation in a changing world. *Global Change Biology*, 25(11), 3625-3641. <https://doi.org/10.1111/gcb.14756>
- Lavergne, S., Mouquet, N., Thuiller, W., & Ronce, O. (2010). Biodiversity and Climate Change: Integrating Evolutionary and Ecological Responses of Species and Communities. *Annual Review of Ecology, Evolution, and Systematics*, 41(1), 321-350. <https://doi.org/10.1146/annurev-ecolsys-102209-144628>
- Leibold, M. A., & Chase, J. M. (2017). *Metacommunity Ecology, Volume 59*. Princeton University Press.
- Leibold, M. A., Holyoak, M., Mouquet, N., Amarasekare, P., Chase, J. M., Hoopes, M. F., Holt, R. D., Shurin, J. B., Law, R., Tilman, D., Loreau, M., & Gonzalez, A. (2004). The metacommunity concept: A framework for multi-scale community ecology. *Ecology Letters*, 7(7), 601-613. <https://doi.org/10.1111/j.1461-0248.2004.00608.x>
- Lenoir, J., Gégout, J. C., Marquet, P. A., Ruffray, P. de, & Brisse, H. (2008). A Significant Upward Shift in Plant Species Optimum Elevation During the 20th Century. *Science*, 320(5884), 1768-1771. <https://doi.org/10.1126/science.1156831>
- Lenoir, J., & Svenning, J.-C. (2015). Climate-related range shifts - a global multidimensional synthesis and new research directions. *Ecography*, 38(1), 15-28. <https://doi.org/10.1111/ecog.00967>
- Loarie, S. R., Duffy, P. B., Hamilton, H., Asner, G. P., Field, C. B., & Ackerly, D. D. (2009). The velocity of climate change. *Nature*, 462(7276), 1052-1055. <https://doi.org/10.1038/nature08649>
- Martin, G., Devictor, V., Motard, E., Machon, N., & Porcher, E. (2019). Short-term climate-induced change in French plant communities. *Biology Letters*, 15(7), 20190280. <https://doi.org/10.1098/rsbl.2019.0280>
- Merle, H., Garmendia, A., Hernández, H., & Ferriol, M. (2020). Vegetation change over a period of 46 years in a Mediterranean mountain massif (Penyagolosa, Spain). *Applied Vegetation Science*, 23(4), 495-507. <https://doi.org/10.1111/avsc.12507>
- Microsoft, & Weston, S. (2022). *foreach: Provides Foreach Looping Construct*. <https://CRAN.R-project.org/package=foreach>
- Mori, A. S., Isbell, F., & Seidl, R. (2018). B-Diversity, Community Assembly, and Ecosystem Functioning. *Trends in Ecology & Evolution*, 33(7), 549-564. <https://doi.org/10.1016/j.tree.2018.04.012>
- Olden, J. D., & Rooney, T. P. (2006). On defining and quantifying biotic homogenization. *Global Ecology and Biogeography*, 15(2), 113-120. <https://doi.org/10.1111/j.1466-822X.2006.00214.x>
- OpenStreetMap contributors. (2017). *Planet dump retrieved from https://planet.osm.org*.

- Ozinga, W. A., Römermann, C., Bekker, R. M., Prinzing, A., Tamis, W. L. M., Schaminée, J. H. J., Hennekens, S. M., Thompson, K., Poschlod, P., Kleyer, M., Bakker, J. P., & van Groenendael, J. M. (2009). Dispersal failure contributes to plant losses in NW Europe. *Ecology Letters*, *12*(1), 66-74. <https://doi.org/10.1111/j.1461-0248.2008.01261.x>
- Pebesma, E. (2018). Simple Features for R: Standardized Support for Spatial Vector Data. *The R Journal*, *10*(1), 439-446. <https://doi.org/10.32614/RJ-2018-009>
- Pérez-Navarro, M. Á., Serra-Díaz, J. M., Svenning, J., Esteve-Selma, M. Á., Hernández-Bastida, J., & Lloret, F. (2021). Extreme drought reduces climatic disequilibrium in dryland plant communities. *Oikos*. <https://doi.org/10.1111/oik.07882>
- Piedallu, C., Chéret, V., Denux, J. P., Perez, V., Azcona, J. S., Seynave, I., & Gégout, J. C. (2019). Soil and climate differently impact NDVI patterns according to the season and the stand type. *Science of The Total Environment*, *651*, 2874-2885. <https://doi.org/10.1016/j.scitotenv.2018.10.052>
- R Core Team. (2019). *R: A Language and Environment for Statistical Computing*. R Foundation for Statistical Computing. <https://www.R-project.org/>
- Reu, J. C., Catano, C. P., Spasojevic, M. J., & Myers, J. A. (2022). Beta diversity as a driver of forest biomass across spatial scales. *Ecology*, *103*(10). <https://doi.org/10.1002/ecy.3774>
- Rey, D., & Neuhäuser, M. (2011). Wilcoxon-Signed-Rank Test. In M. Lovric (Ed.), *International Encyclopedia of Statistical Science* (pp. 1658-1659). Springer. https://doi.org/10.1007/978-3-642-04898-2_616
- Richard, B., Dupouey, J.-L., Corcket, E., Alard, D., Archaux, F., Aubert, M., Boulanger, V., Gillet, F., Langlois, E., Macé, S., Montpied, P., Beaufils, T., Begeot, C., Behr, P., Boissier, J.-M., Camaret, S., Chevalier, R., Decocq, G., Dumas, Y., ... Lenoir, J. (2021). The climatic debt is growing in the understorey of temperate forests: Stand characteristics matter. *Global Ecology and Biogeography*, *n/a*(n/a). <https://doi.org/10.1111/geb.13312>
- Rolland, C. (2003). Spatial and Seasonal Variations of Air Temperature Lapse Rates in Alpine Regions. *Journal of Climate*, *16*(7), 1032-1046. [https://doi.org/10.1175/1520-0442\(2003\)016<1032:SASVOA>2.0.CO;2](https://doi.org/10.1175/1520-0442(2003)016<1032:SASVOA>2.0.CO;2)
- Sala, O. E., Chapin, F. S., Armesto, J. J., Berlow, E., Bloomfield, J., Dirzo, R., Huber-Sanwald, E., Huenneke, L. F., Jackson, R. B., Kinzig, A., Leemans, R., Lodge, D. M., Mooney, H. A., Oesterheld, M., Poff, N. L., Sykes, M. T., Walker, B. H., Walker, M., & Wall, D. H. (2000). Global biodiversity scenarios for the year 2100. *Science (New York, N.Y.)*, *287*(5459), 1770-1774. <https://doi.org/10.1126/science.287.5459.1770>
- Sanczuk, P., De Lombaerde, E., Haesen, S., Van Meerbeek, K., Luoto, M., Van der Veken, B., Van Beek, E., Hermy, M., Verheyen, K., Vangansbeke, P., & De Frenne, P. (2022). Competition mediates understorey species range shifts under climate change. *Journal of Ecology*, *110*(8), 1813-1825. <https://doi.org/10.1111/1365-2745.13907>

- Serra-Diaz, J. M., Franklin, J., Ninyerola, M., Davis, F. W., Syphard, A. D., Regan, H. M., & Ikegami, M. (2014). Bioclimatic velocity: The pace of species exposure to climate change. *Diversity and Distributions*, *20*(2), 169-180. <https://doi.org/10.1111/ddi.12131>
- Socolar, J. B., Gilroy, J. J., Kunin, W. E., & Edwards, D. P. (2016). How Should Beta-Diversity Inform Biodiversity Conservation? *Trends in Ecology & Evolution*, *31*(1), 67-80. <https://doi.org/10.1016/j.tree.2015.11.005>
- Staude, I. R., Pereira, H. M., Daskalova, G. N., Bernhardt-Römermann, M., Diekmann, M., Pauli, H., Van Calster, H., Vellend, M., Bjorkman, A. D., Brunet, J., De Frenne, P., Hédli, R., Jandt, U., Lenoir, J., Myers-Smith, I. H., Verheyen, K., Wipf, S., Wulf, M., Andrews, C., ... Baeten, L. (2022). Directional turnover towards larger-ranged plants over time and across habitats. *Ecology Letters*, *25*(2), 466-482. <https://doi.org/10.1111/ele.13937>
- Steinbauer, M. J., Grytnes, J.-A., Jurasinski, G., Kulonen, A., Lenoir, J., Pauli, H., Rixen, C., Winkler, M., Bardy-Durchhalter, M., Barni, E., Bjorkman, A. D., Breiner, F. T., Burg, S., Czortek, P., Dawes, M. A., Delimat, A., Dullinger, S., Erschbamer, B., Felde, V. A., ... Wipf, S. (2018). Accelerated increase in plant species richness on mountain summits is linked to warming. *Nature*, *556*(7700), Article 7700. <https://doi.org/10.1038/s41586-018-0005-6>
- Suggitt, A. J., Wilson, R. J., Isaac, N. J. B., Beale, C. M., Auffret, A. G., August, T., Bennie, J. J., Crick, H. Q. P., Duffield, S., Fox, R., Hopkins, J. J., Macgregor, N. A., Morecroft, M. D., Walker, K. J., & Maclean, I. M. D. (2018). Extinction risk from climate change is reduced by microclimatic buffering. *Nature Climate Change*, *8*(8), Article 8. <https://doi.org/10.1038/s41558-018-0231-9>
- Svenning, J.-C., & Sandel, B. (2013). Disequilibrium vegetation dynamics under future climate change. *American Journal of Botany*, *100*(7), 1266-1286. <https://doi.org/10.3732/ajb.1200469>
- Tatsumi, S., Iritani, R., & Cadotte, M. W. (2021). Temporal changes in spatial variation: Partitioning the extinction and colonisation components of beta diversity. *Ecology Letters*. <https://doi.org/10.1111/ele.13720>
- Tatsumi, S., Iritani, R., & Cadotte, M. W. (2022). Partitioning the temporal changes in abundance-based beta diversity into loss and gain components. *Methods in Ecology and Evolution*, *13*(9), 2042-2048. <https://doi.org/10.1111/2041-210X.13921>
- Tobias, N., & Monika, W. (2012). Does taxonomic homogenization imply functional homogenization in temperate forest herb layer communities? *Plant Ecology*, *213*(3), 431-443. <https://doi.org/10.1007/s11258-011-9990-3>
- Vangansbeke, P., Máliš, F., Hédli, R., Chudomelová, M., Vild, O., Wulf, M., Jahn, U., Welk, E., Rodríguez-Sánchez, F., & Frenne, P. D. (2021). ClimPlant: Realized climatic niches of vascular plants in European forest understoreys. *Global Ecology and Biogeography*, *30*(6), 1183-1190. <https://doi.org/10.1111/geb.13303>

- Vittoz, P., & Engler, R. (2007). Seed dispersal distances: A typology based on dispersal modes and plant traits. *Botanica Helvetica*, 117(2), 109-124.
<https://doi.org/10.1007/s00035-007-0797-8>
- Wang, S., Loreau, M., Mazancourt, C., Isbell, F., Beierkuhnlein, C., Connolly, J., Deutschman, D. H., Doležal, J., Eisenhauer, N., Hector, A., Jentsch, A., Kreyling, J., Lanta, V., Lepš, J., Polley, H. W., Reich, P. B., Ruijven, J., Schmid, B., Tilman, D., ... Craven, D. (2021). Biotic homogenization destabilizes ecosystem functioning by decreasing spatial asynchrony. *Ecology*, 102(6).
<https://doi.org/10.1002/ecy.3332>
- Whittaker, R. H. (1960). Vegetation of the Siskiyou Mountains, Oregon and California. *Ecological Monographs*, 30(3), 279-338. <https://doi.org/10.2307/1943563>
- Wickham, H. (2011). Ggplot2. *WIREs Computational Statistics*, 3(2), 180-185.
<https://doi.org/10.1002/wics.147>
- Xu, W.-B., Blowes, S. A., Brambilla, V., Chow, C. F. Y., Fontrodona-Eslava, A., Martins, I. S., McGlenn, D., Moyes, F., Sagouis, A., Shimadzu, H., van Klink, R., Magurran, A. E., Gotelli, N. J., McGill, B. J., Dornelas, M., & Chase, J. M. (2023). Regional occupancy increases for widespread species but decreases for narrowly distributed species in metacommunity time series. *Nature Communications*, 14(1), Article 1.
<https://doi.org/10.1038/s41467-023-37127-2>
- Zellweger, F., De Frenne, P., Lenoir, J., Vangansbeke, P., Verheyen, K., Bernhardt-Römermann, M., Baeten, L., Hédli, R., Berki, I., Brunet, J., Van Calster, H., Chudomelová, M., Decocq, G., Dirnböck, T., Durak, T., Heinken, T., Jaroszewicz, B., Kopecký, M., Máliš, F., ... Coomes, D. (2020). Forest microclimate dynamics drive plant responses to warming. *Science*, 368(6492), 772-775.
<https://doi.org/10.1126/science.aba6880>
- Zuur, A. F., Ieno, E. N., & Elphick, C. S. (2010). A protocol for data exploration to avoid common statistical problems. *Methods in Ecology and Evolution*, 1(1), 3-14.
<https://doi.org/10.1111/j.2041-210X.2009.00001.x>
- Zwiener, V. P., Lira-Noriega, A., Grady, C. J., Padiál, A. A., & Vitule, J. R. S. (2018). Climate change as a driver of biotic homogenization of woody plants in the Atlantic Forest. *Global Ecology and Biogeography*, 27(3), 298-309.
<https://doi.org/10.1111/geb.12695>